

CURRENT DRIVE BY ASYMMETRICAL HEATING IN A TOROIDAL PLASMA

by

JOHN MICHEL GAHL, B.S. in E.E., M.S. in E.E.

A DISSERTATION

IN

ELECTRICAL ENGINEERING

Submitted to the Graduate Faculty
of Texas Tech University in
Partial Fulfillment of
the Requirements for
the Degree of

DOCTOR OF PHILOSOPHY

~~Approved~~

August, 1986

10/1
1976
No. 53
204.3

ACKNOWLEDGMENTS

I would like to thank Dr. M. Kristiansen, Dr. Marion Hagler, and Dr. Osamu Ishihara for their guidance and advice on this project. The education I have recieved from them over the past several years is greatly appreciated. I would also like to thank Dr. Lynn Hatfield and Dr. John Walkup for serving on my committee. And finally, I gratefully acknowledge the financial support of the National Science Foundation for my research.

TABLE OF CONTENTS

ACKNOWLEDGMENTS	ii
ABSTRACT	v
LIST OF FIGURES	vi
I. INTRODUCTION	1
II. THEORETICAL CONSIDERATIONS	8
Current Drive by Heating of Minority Species Ions as Proposed by Fisch	8
Corrections to Fisch's Theory Necessary for Small Tokamaks	17
Difficulties in the Preferential Depositon of RF Power into Particles Participating in Current Drive	21
Current Drive by Asymmetrical Heating of a One Ion Species Plasma	26
Dispersion Relation of the Fast Alfvén Wave in a Hydrogen Plasma Near the Fundamental Cyclotron Frequency	33
III. EXPERIMENTAL APPARATUS AND PROCEDURE	52
Tokamak and Associated Equipment	52
Slow Wave Antenna	57
Method of Determination of Current Generation	65
IV. RESULTS	76
General Results	76
Analysis of Results	80

V. CONCLUSIONS	85
A General Assessment of Current Drive by Asymmetrical Heating of Ions.	85
Peculiarities of Current Drive by Asymmetrical Heating of Ions Which Warrant Further Investigation	89
LIST OF REFERENCES.	92
APPENDIX A: DEFINITION OF THE SAFETY FACTOR.	95
APPENDIX B: DEFINITION OF THE SLOWING DOWN RATE	96

ABSTRACT

This report describes the first experimental observation of current generation by asymmetrical heating of ions. A unidirectional fast Alfvén wave launched by a slow wave antenna inside the Texas Tech Tokamak, asymmetrically heated the ions. Measurements of the asymmetry of the toroidal plasma current with probes at the top and bottom of the toroidal plasma column confirmed the current generation indirectly. Current generation, obtained in a one-species, hydrogen plasma, is a phenomenon which had not been predicted previously. Calculations of the dispersion relation for the fast Alfvén wave near the fundamental cyclotron resonance in a one-species, hydrogen plasma, using warm plasma theory, support the experimental results.

LIST OF FIGURES

Figures

1.	Diagram Showing Displacement of Particles in Velocity Space.	9
2.	Cross Section of Tokamak, Showing Value of the Cyclotron Resonance Frequency for He ³ at Plasma Edges.	23
3.	Cross Section of Tokamak, Showing Area of Asymmetrical Heating with Edge of Plasma Satisfying $\omega = \Omega_L + 4V_{T\alpha} k_{\parallel}$	24
4.	Cross Section of Tokamak, Showing Area of Asymmetrical Heating. Particles Satisfying $\omega = \Omega_L + k_{\parallel} W V_{T\alpha}$ are Moving into the Page, Particles Satisfying $\omega = \Omega_L - k_{\parallel} W V_{T\alpha}$ are Moving out of the Page.	28
5.	Cross section of Tokamak, Showing Area of Asymmetrical Heating and Area Where Wave is Unable to Propagate.	50
6.	Top View of Texas Tech Tokamak Vacuum Chamber.	54
7.	Block Diagram of the Texas Tech Tokamak Facility	56
8.	Original Slow Wave Antenna Assembly.	59
9.	Stainless Steel Tray and Coiled Slow Wave Structure of Original Antenna.	60
10.	Phase Comparator Circuitry.	64
11.	Photograph of Long Slow Wave Antenna.	66
12.	Diagram of Long Slow Wave Antenna.	67
13.	Cross Section of Long Slow Wave Antenna.	68

14.	Section of Tokamak Plasma Showing Area of Asymmetrical Heating, Area of Wave Cut-off, Areas of RF Current Generation, Direction of I_{OH} (Ohmic Heating Current), and Rotational Transform of the Machine (Which is Exaggerated for Purposes of Demonstration).	70
15.	Section of Tokamak Showing Location of Current Probes in Relation to Plasma Column.	72
16.	Top View of Texas Tech Tokamak Vacuum Chamber With Relative Position of Long Antenna and \dot{B} Probes.	74
17.	Typical Experimental Data, Probe Signal 'A'-'B', Which Depicts Asymmetry of Current Density in Plasma Column. RF at 9.7 MHz Places Heating Layer 'Outside' Machine, RF at 7.7 MHz Places Heating Layer 'Inside' Machine.	77
18.	Probe Signal 'A'-'B', Plotted as a Function of Frequency.	79
19.	Probe Signal 'A'-'B' During Tokamak Discharge in Which RF Was Modulated Between 7.5 and 8.1 MHz.	81
20.	Cross Section of a Tokamak Showing Current Drive by Asymmetrical Heating of Ions Flattening the Current Density Profile of a Tokamak Plasma Column.	91

CHAPTER I

INTRODUCTION

A tokamak is a device which confines a toroidal plasma in a magnetic bottle. By passing an electric, toroidal current through the plasma, a poloidal magnetic field is created within the plasma. This field, in combination with a strong toroidal magnetic field generated by external coils, confines the plasma. When confined, a plasma of light ions can then be heated, hopefully to the point where a fraction of the nuclei overcome mutual electrostatic repulsion, and fuse, releasing energy.

The toroidal electric current needed in tokamaks to maintain confinement is almost always coupled inductively into the tokamaks, and therefore is driven only for a limited amount of time. If the tokamak is to become a usable fusion reactor however, it should be operated in the steady state, thereby avoiding possibly destructive thermal stresses in the reactor. Therefore, there is a need for devising a method of steady state current generation in tokamaks.

A variety of steady state current drive schemes have been suggested. Most of these schemes involve imparting

momentum to electrons, either with neutral particle beams or waves launched in the plasma^{1,2,3}.

In a scheme suggested by Ohkawa², a beam of neutral particles, with an atomic number higher than that of the ions in the plasma, is injected tangentially into the plasma column. The particles must be neutral so that they are not deflected by the strong magnetic field of the tokamak. Once in the plasma, the atoms in the beam are quickly ionized. These ions, having a larger charge state than the background ions, collide more frequently with the electrons. Therefore, this beam of recently ionized atoms "drags" electrons with it, imparting momentum to the electrons and driving an electron current. Current drive has indeed been achieved using this scheme⁴. Unfortunately, the technology required to drive a high power neutral particle beam is difficult and expensive. Beyond this, there is great doubt whether neutral particle beam drivers, which are delicate devices, can withstand the environment of a working fusion reactor.

Another scheme which has received experimental attention⁵ was suggested by Fisch³. This scheme uses waves in the frequency range of lower hybrid to impart momentum to high velocity electrons traveling in one direction around the tokamak and hence drive an electron current. To insure that no momentum is imparted to the ions, which would be counterproductive, it is necessary to maintain

$\omega/k_{\parallel} = V_{\text{Phase}} \gg V_{\text{Ti}}$ (where ω is the frequency of the wave, k_{\parallel} is its parallel wave number, V_{Phase} is the phase velocity of the wave, and V_{Ti} is the ion thermal velocity). This condition requires relatively high frequency RF power (a few GHz in large machines). Unfortunately, extremely high power RF technology in this frequency range is still experimental in nature, and far from being a mature technology. Furthermore, experimental results suggest that this scheme's efficiency falls short of that required for a fusion reactor.⁶ In any case, it seems likely that the high plasma density of such fusion reactors will prevent the use of lower hybrid waves.⁷

In 1981, Fisch proposed yet another current drive scheme.⁸ This scheme differs from others in that RF waves interact with ions rather than electrons and in that the RF waves need not inject net toroidal momentum into the plasma.

Fisch proposed that a fast Alfvén wave be launched in one direction around a tokamak containing a two ion species plasma. The frequency of the wave would be chosen, considering the Doppler shift, so that the wave would cyclotron-damp preferentially into high-speed minority ions moving around the torus in the same direction as the wave. This condition causes the minority species particles moving in the direction of the wave to become hotter and hence to collide less frequently with the majority ions than the

minority particles streaming in the opposite direction. Therefore, the minority ion species drift with respect to the majority ions.

If the minority ions carry a different charge than the majority ions, then a toroidal current results, unless the electrons move in such a way as to cancel it. To see that this is not the case, we recall that in a neutral plasma the total current is frame invariant. Therefore, we can choose a reference frame in which the total ion current is zero. Note that both ion species move with respect to this frame. Because the electrons collide more frequently with the ions having a larger electric charge, the electrons experience a net ion drag and therefore drift and produce a net current. In fact, Fisch predicted that a net current carried mainly by the electrons would be produced because the relatively few minority ions, streaming with respect to the majority ions, have a larger electric charge than the majority ions, and therefore pull the electrons along with them.

This use of fast Alfvén waves to drive current, is attractive from a technological point of view. To launch Alfvén waves, relatively low frequency RF power (a few to some tens of MHz in large machines) is required. High power RF technology at this frequency is a mature technology, developed for radio broadcast. Therefore, it would appear that there should be great interest in the experimental

investigation of this current drive scheme. In fact, the original focus of the research presented here was the experimental investigation of current drive by asymmetrical heating of a minority species using unidirectional Alfvén waves.

Upon closer scrutiny, Fisch's original proposal⁷ contained assumptions which are perhaps proper for large reactor type machines, but are certainly improper in small tokamaks like the Texas Tech Tokamak, the machine on which this research was to be conducted on. Also, Fisch does not deal with the problem of insuring that RF power is delivered preferentially to the particles participating in current drive, instead of to the bulk ions.

These difficulties led to the development of a new type of current drive scheme. This scheme is very similar to Fisch's original scheme, but differs in that only one species of ions, hydrogen, is used. It was with this scheme that current drive by asymmetrical heating of a hydrogen plasma by unidirectional Alfvén waves, was demonstrated experimentally for the first time in this work.

In the interest of logical progression, the order of the dissertation generally follows the path taken in the research. The following is a brief description of the contents of the ensuing chapters.

Chapter 2 contains theoretical considerations. Within it there is a description of Fisch's theory, and an

extension of that theory to include effects Fisch did not consider. Difficulties in the preferential deposition of RF power into particles participating in current drive and the resulting ramifications are explored. Due to these effects, the new type of current drive, current drive by asymmetrical heating of a hydrogen plasma by unidirectional Alfvén waves, is presented. Included in the presentation of this one species current drive scheme is a numerical calculation of the dispersion relation of the fast wave near the fundamental cyclotron resonance frequency, a calculation useful in understanding the one species current drive effect.

Chapter 3 presents a description of the experiment that was conducted to detect this current drive effect. This chapter includes a short description of the tokamak itself, and its supporting equipment. There is also a description of the slow wave antenna used to launch unidirectional fast Alfvén waves in the tokamak.

Chapter 4 gives the results and analysis of the experiments. The theoretical efficiency of current drive in the Texas Tech Tokamak is calculated from the theory developed previously. The results of the experiment and the results of the calculation are compared.

Chapter 5, "Conclusions," contains an assessment of the practicality of the one species current drive scheme in general. This chapter also contains a theoretical

prediction of the performance and practicality of the one species current drive scheme in a particular large tokamak, JET, the Joint European Torus. Finally, peculiarities of this current drive scheme which may warrant further investigation are discussed.

CHAPTER II
THEORETICAL CONSIDERATIONS

Current Drive by Heating of Minority
Species Ions as Proposed by Fisch

The following is a description of Fisch's scheme of current generation by minority species heating⁸ including 1) his calculation of the amount of power that is necessary to establish a minority species ion drift and his calculation of the electric current that results from this ion drift, and 2) his calculation of which minority species ions should be heated so as to optimize current generation (those ions being minority species ions with a particular parallel velocity) is also included.

Fisch first assumes that some means exists to displace a velocity space element of volume Δf from the velocity space location labeled 1 to the velocity space location labeled 2 (see Fig. 1). He assumes that momentum in the z direction (the direction parallel to the magnetic field) is lost from the minority species ions in location 1 at a rate v_1 while the minority ions in location 2 lose momentum in the z direction at a rate v_2 . Fisch then states that the amount of energy required to displace ions from location 1 to location 2 is simply

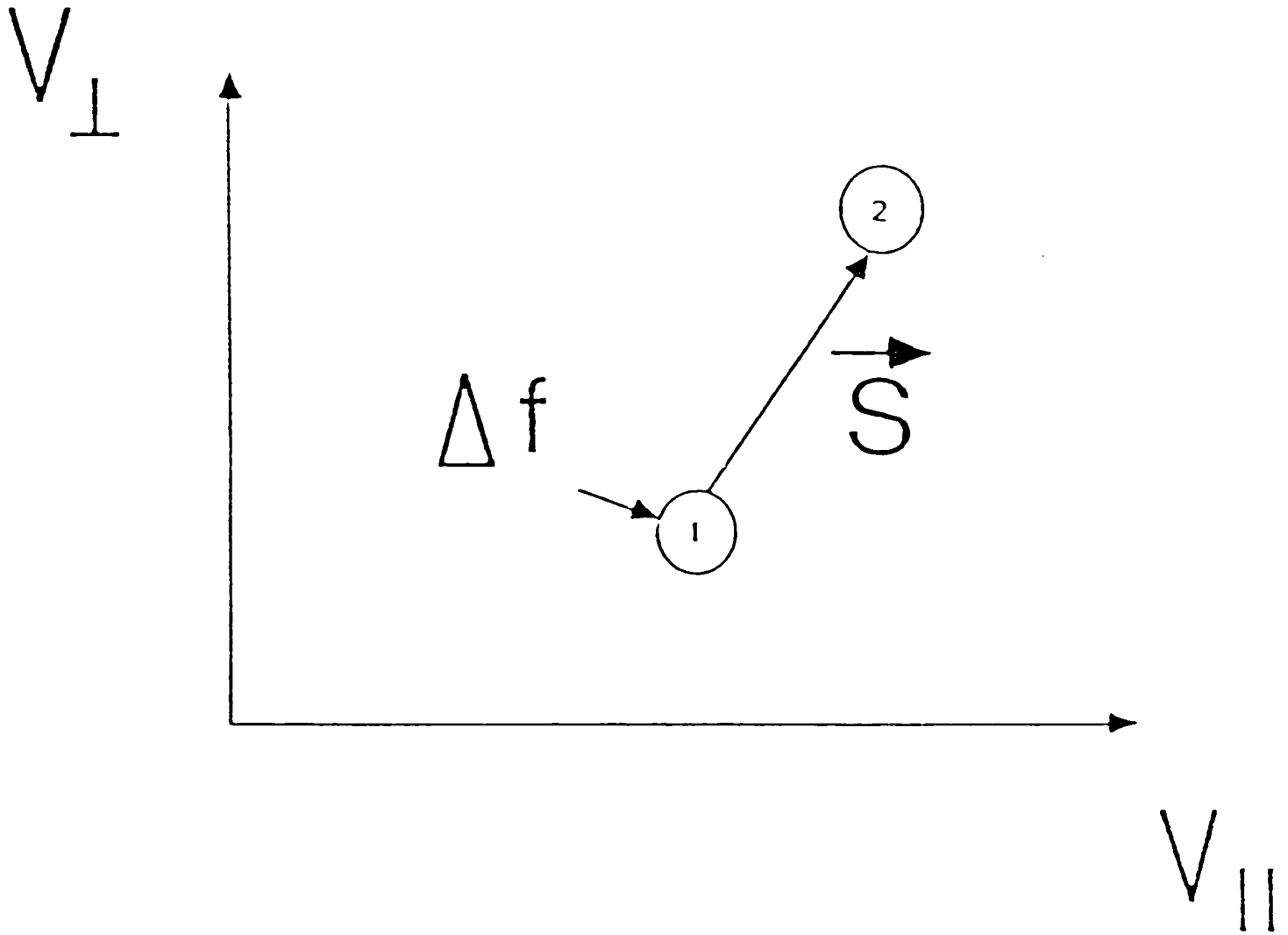


Fig. 1 Diagram Showing Displacement of Particles in Velocity Space.

$$\Delta E = (E_2 - E_1) \delta f \quad (1)$$

$$E_j = m_\alpha V_j^2 / 2, \quad (2)$$

where V_j is the speed of the ions at location j and m_α is the mass of a minority species ion.

The change in parallel momentum in the minority species induced by this displacement is given approximately by

$$\Delta p_z \approx \delta f m_\alpha [V_{z2} \exp(-\nu_2 t) - V_{z1} \exp(-\nu_1 t)], \quad (3)$$

where V_{z2} is the velocity, in the z direction, of the minority ions at location 2, and V_{z1} is the velocity, in the z direction, of the minority ions at location 1. From this change in parallel momentum, Fisch finds the directed momentum of the minority species, time-averaged over a time Δt , as

$$\begin{aligned} p_\alpha &= \frac{1}{\Delta t} \int_0^{\Delta t} \Delta p_z dt \\ &= \frac{m_\alpha \delta f}{\Delta t} \left[\frac{V_{z2}}{\nu_2} - \frac{V_{z1}}{\nu_1} \right], \quad (4) \end{aligned}$$

where he obtains the second equality by assuming Δt is large compared to $1/\nu_1$ and $1/\nu_2$.

Fisch then defines the rate at which power is dissipated to maintain the directed momentum as simply

$$P_d = \Delta E / \Delta t. \quad (5)$$

Then, combining Eqs. (1),(4) and (5), he finds the ratio of minority species momentum to power dissipated as

$$\frac{p_\alpha}{P_d} = m_\alpha \left[\frac{V_{z2}/v_2 - V_{z1}/v_1}{E_2 - E_1} \right]. \quad (6)$$

Then, defining \vec{s} as the velocity space vector that represents the displacement from location 1 to location 2, and taking the limit $|\vec{s}| \rightarrow 0$ in Eq. (6), he finds

$$\frac{p_\alpha}{P_d} = m_\alpha \left[\frac{\hat{s} \cdot \nabla (V_z/v)}{\hat{s} \cdot \nabla E} \right]. \quad (7)$$

From Eq.(7), it is obvious that a minority species drift occurs only if

$$\hat{s} \cdot \nabla (V_z/v) \neq 0 ,$$

which is true if

$$\hat{s} \cdot \nabla V_z \neq 0 \quad (8)$$

or

$$\hat{s} \cdot \nabla v \neq 0 \quad (9)$$

When Eq. (8) holds, momentum is injected into the minority

species ions, and current generation is achieved in a manner similar to earlier current drive schemes^{2,3}. However, if Eq.(9) holds and Eq.(8) does not, minority species drift still occurs, but with no momentum injection. By asymmetrical perpendicular heating, particular minority ions can be moved to a region of velocity space where they possess a lower collision frequency. This movement in velocity space, corresponding to Eq.(9) being satisfied, generates a minority ion drift, and since electric current arises from the motion of electrons reacting to the relative drift between the two ion species, an electric current is generated. It is this current drive scheme, current drive without momentum injection, or current drive by minority species heating, that Fisch investigates.

To consider quantitatively the amount of current generated, Fisch assumes that

$$v = v_e + v_i \quad (10)$$

where v_e and v_i are the rates of momentum loss of the minority ions to the electrons and the majority ions, respectively. He also assumes the velocity of the heated ions, V , is of course lower than the electron velocity, but greater than the velocity of the bulk ions. Using these assumptions, and assuming that no momentum was injected into the plasma, or

$$\hat{s} \cdot \nabla V_z = 0 ,$$

Fisch finds

$$\frac{P_\alpha}{P_d} = \frac{3}{2} m_\alpha V_z \left[\frac{v_i}{v} \right] \left[\frac{1}{vE} \right]. \quad (11)$$

It is now possible to calculate the amount of current generated per unit power dissipated. Fisch assumes that the minority ion species drifts at a speed V_α parallel to the magnetic field while the majority ion species drifts at a speed V_i . He assumes that the minority ion charge state is Z_α while the majority ion charge state is assumed to be unity. Then, since the electrons collide with the minority ions Z_α^2 times more often than with the majority ions, the electron parallel drift speed, V_e , must obey, in the steady state,

$$n_\alpha Z_\alpha^2 (V_\alpha - V_e) + n_i (V_i - V_e) = 0 , \quad (12)$$

where n_α and n_i are, respectively, the minority and majority ion densities. He also assumes that no momentum is injected into the plasma,

$$n_\alpha m_\alpha V_\alpha + n_i m_i V_i + n_e m_e V_e = 0 , \quad (13)$$

and that charge neutrality is obeyed,

$$Z_{\alpha} n_{\alpha} + n_i - n_e = 0 . \quad (14)$$

The current is given as

$$J = e(-n_e V_e + Z_{\alpha} n_{\alpha} V_{\alpha} + n_i V_i) \quad (15)$$

so that combining Eqs. (12)-(15) and taking the limit $m_e/m_i \rightarrow 0$, he obtains

$$J = \frac{en_{\alpha} V_{\alpha} (1-Z_{\alpha})}{n_i + n_{\alpha} Z_{\alpha}^2} \left[Z_{\alpha} n_i + (n_e - n_i) \frac{m_{\alpha}}{m_i} \right] . \quad (16)$$

Assuming the regime

$$n_{\alpha} Z_{\alpha}^2 \ll n_i \approx n_e$$

and using Eqs.(16) and (11), Fisch finally finds

$$\frac{J}{P_d} = \frac{3}{2} eV_z (Z_{\alpha} - Z_{\alpha}^2) \frac{v_i}{v_E^2} . \quad (17)$$

In an attempt to normalize this relation, Fisch adopted several normalizations and definitions, most of which are characteristic of previous work^{2,3,9}. He normalizes J to

$-enV_{Te}$ and P_d to $v_o n_e m_e V_{Te}^2$, (where $v_o = \omega_{pe}^4 \ln \Lambda / 2\pi n_o V_{Te}^3$).

He then defines the quantities

$$W = V_z / V_{T\alpha} \quad (18)$$

$$U = V / V_{T\alpha} \quad (19)$$

$$Y = v_e / v_i U^3 \quad (20)$$

or

$$Y = \frac{1}{3} \left[\frac{2}{\pi} \right]^{1/2} \left[\frac{m_e}{m_\alpha} \right]^{1/2} \left[\frac{1}{1 + (m_\alpha / m_i)} \right]$$

and specifies v_e and v_i as⁹

$$v_i = v_o Z_\alpha^2 [m_e / m_\alpha]^2 [1 + (m_\alpha / m_i)] [V_{Te}^3 / V^3] \quad (21)$$

$$v_e = v_o Z_\alpha^2 [2/9\pi]^{1/2} [m_e / m_\alpha]^2 [1 + (m_\alpha / m_e)]. \quad (22)$$

Using these normalizations and defined quantities, Fisch finds the normalized relation for J/P_d as

$$J/P_d = \frac{3WU}{(1+YU^3)^2} \left[\frac{1 - Z_\alpha^{-1}}{1 + (m_\alpha / m_i)} \right]. \quad (23)$$

Finally, Fisch gives a simple expression for the efficiency of his current drive scheme. This expression can be easily maximized as a function of W , since, as we will see, its maximum occurs for $W > 1$, a region where $W \approx U$. He

found that the current drive efficiency, J/P_d , is maximized if

$$W = W_o = (2Y)^{-1/3} . \quad (24)$$

Because W (see Eq.(18)) is simply the ratio of the parallel velocity of the minority species ions that are heated to the bulk thermal velocity of the minority species, maximizing the relation for J/P_d as a function of W is the same as calculating which minority-species ions should be heated so as to optimize current generation.

Therefore, for a given combination of majority and minority ion species, Eqs.(20) and (24) tell the experimenter which minority species ions to heat (ions with a particular parallel velocity). Upon heating these ions, the experimenter can use Eq.(23) to determine how much current drive to expect.

Within his paper, Fisch calculates the expected current drive efficiency of his scheme in a large tokamak, similar to the PLT tokamak at Princeton University¹⁰. With a combination of minority and majority ion species that would result in $W \approx 5$, Fisch predicts that about two watts of RF power would be needed to drive each amp of toroidal current. If this prediction proved to be true, this current drive scheme would be of great interest to tokamak researchers.

Corrections to Fisch's Theory Necessary
for Small Tokamaks

When our experiment was first proposed it was assumed that Fisch's theory as just presented would hold in small tokamaks like the Texas Tech Tokamak. A plasma with a majority species of deuterium and a minority species of helium-3 was to be used in our experiment, due to previous experimental data which showed that the fast Alfvén wave is able to propagate near the ion-cyclotron resonance of helium-3 in the Texas Tech Tokamak¹¹, thus enabling the heating of this minority species. Using this combination of ions species, we can find by using Eqs.(20) and (24) that $W_0 \approx 7$. In other words, current generation would be optimized if RF energy were imparted to those minority species ions moving around the tokamak at about seven times the ion thermal velocity. If RF energy were to be imparted to these ions, then using Eq.(23) and knowing the geometry of the Texas Tech Tokamak (which is described in Chapter 3) we find the efficiency of current drive to be 0.172 amps of toroidal current drive for each watt of RF energy used.

Unfortunately, upon closer scrutiny of his paper, it becomes apparent that Fisch makes several approximations which are perhaps applicable in large reactor type tokamaks, but are certainly inapplicable in small tokamaks, such as the Texas Tech Tokamak. In fact, two of the assumptions,

which we now explore, are inapplicable in virtually all existing tokamaks.

It is now clear to us that Fisch assumes that the electron temperature, T_e , equals the minority ion species temperature T_α . The importance of this becomes clear if we reexamine his quantity, Y ,

$$Y = v_e/v_i U^3 \quad (20)$$

or

$$Y = \frac{1}{3} \left[\frac{2}{\pi} \right]^{1/2} \left[\frac{m_e}{m_\alpha} \right]^{1/2} \left[\frac{1}{1 + (m_\alpha/m_i)} \right].$$

If we assume that $T_\alpha \neq T_e$, the quantity Y , defined in the same way as in Eq.(20), becomes

$$Y = v_e/v_i U^3 \quad (25)$$

or

$$Y = \frac{1}{3} \left[\frac{2}{\pi} \right]^{1/2} \left[\frac{m_e}{m_\alpha} \right]^{1/2} \left[\frac{1}{1 + (m_\alpha/m_i)} \right] \left[\frac{T_\alpha}{T_e} \right]^{3/2}$$

In the Texas Tech Tokamak, $T_e \approx 100$ eV and $T_\alpha \approx 20$ eV. If we use these values in Eqs.(24) and (25), we find a corrected value for the optimized value of W , which is $W_0 \approx 15.7$. In other words, current generation would be optimized if RF energy were imparted to those minority species ions moving around the tokamak at about 15.7 times

the minority ion thermal velocity. It is, therefore, obvious to us that current cannot be optimally driven in our machine, since there are virtually no particles with velocities 15.7 times the minority ion thermal velocity.

A particle velocity much more likely to exist in the Texas Tech Tokamak is $V_z \approx 4V_{T\alpha}$,¹² that is, it is much more likely that the experimenter can arrange for W to equal 4 than to 15.7. If we use Eqs.(23) and (25), let $W = 4$, $T_e = 100$ eV, $T_\alpha = 20$ eV, and use a plasma with a majority species of deuterium and a minority species of helium-3, the expected efficiency of Fisch's scheme in the Texas Tech Tokamak is approximately 25 milliamps of toroidal current drive for each watt of RF energy used. This efficiency is about seven times lower than the efficiency predicted by Fisch's original calculations.

Another assumption made by Fisch which makes a radical difference in the application of his calculations to real devices is his assumption that the effective charge of the plasma, Z_{eff} , equals unity. In all small machines like the Texas Tech Tokamak, and in fact virtually all large operating tokamaks^{13,14,15}, $Z_{eff} \geq 2$.

If we go back to his calculation and add in the term Z_{eff} , we find that Eq.(12)

$$n_\alpha Z_\alpha^2 (V_\alpha - V_e) + n_i (V_i - V_e) = 0$$

becomes

$$n_{\alpha} Z_{\alpha}^2 (V_{\alpha} - V_e) + n_i Z_{\text{eff}}^2 (V_i - V_e) = 0 \quad (26)$$

and Eq. (15)

$$J = e(-n_e V_e + Z_{\alpha} n_{\alpha} V_{\alpha} + n_i V_i)$$

becomes

$$J = e(-n_e V_e + Z_{\alpha} n_{\alpha} V_{\alpha} + Z_{\text{eff}} n_i V_i) \quad (27)$$

resulting in Eq. (17)

$$\frac{J}{P_d} = \frac{3}{2} e V_z (Z_{\alpha} - Z_{\alpha}^2) \frac{v_i}{v^2 E}$$

becoming

$$\frac{J}{P_d} = \frac{3}{2} e V_z \left[Z_{\alpha} - \frac{Z_{\alpha}^2}{Z_{\text{eff}}} \right] \frac{v_i}{v^2 E} \quad (28)$$

From Eq. (28) we can see that if a tokamak has a hydrogenic plasma with an effective charge of 2, or $Z_{\text{eff}} = 2$, and contains a minority species of He^3 or He, where $Z_{\alpha} = 2$, the efficiency of Fisch's current drive scheme goes to zero. Though we do not know exactly what the effective charge of the Texas Tech Tokamak is (determination of the effective charge of a tokamak plasma is extremely difficult and is not known with great certainty in any machine), if it is as we expect, approximately 2, the efficiency of this current drive scheme in the Texas Tech Tokamak with the originally proposed D- He^3 plasma, could be extremely low indeed. In any case, with any value of Z_{eff}

greater than 1, the efficiency of current drive is smaller than that originally predicted.

Difficulties in the Preferential
Deposition of RF Power into Particles
Participating in Current Drive

Though Fisch was quite explicit in his paper in the description of what minority species ions to heat to achieve a particular current drive efficiency, he gave few clues to the experimenter on how exactly to heat those particular minority species ions. As already mentioned, the basic idea is to couple RF energy from a unidirectional fast Alfvén wave through Doppler shifted ion cyclotron resonance to minority species ions moving with a particular parallel velocity around the tokamak. This quality differentiates his current drive scheme from other current drive schemes in that it results in current generation being spatially localized within the tokamak.

Whereas other current drive effects are bulk effects, asymmetrical heating of minority species ions only occurs for minority species ions that satisfy

$$\omega = \Omega_L + k_{\parallel} W V_{T\alpha} \quad (29)$$

where Ω_L is the local value of the minority ion cyclotron frequency, ω is the frequency of the RF power applied, k_{\parallel} is the parallel wave number of the launched fast Alfvén wave,

and $WV_{T\alpha}$ is some multiple of the minority species thermal velocity (recalling from Eq.(18), that parallel velocity V_z equals $WV_{T\alpha}$). The magnetic field of a tokamak decreases towards the outside of the torus. This characteristic of tokamaks causes the local cyclotron frequency of the minority ions ($\Omega_L = Z_\alpha e |B| / m_\alpha$) to be spatially dependent. In the Texas Tech Tokamak, the local cyclotron frequency for He^3 ranges from approximately 6.7 MHz at the inside edge of the plasma column to 3.7 MHz at the outside edge (see Fig. 2).

Our original experimental plan was to choose an applied frequency, ω , such that the spatial location, where $\omega = \Omega_L$ was satisfied, existed outside the plasma, while the spatial location, where $\omega = \Omega_L + 4V_{T\alpha} k_{\parallel}$ was satisfied, existed just inside the plasma (see Fig. 3). This circumstance would eliminate two undesirable effects. If the spatial location of $\omega = \Omega_L + 4V_{T\alpha} k_{\parallel}$ was just inside the plasma, heating of slower minority ions ($W = 3, 2, 1$ etc.) would be impossible (see Fig. 3). This feature is desirable since these slower ions convert RF energy to current drive less efficiently. The other undesirable effect our original plan eliminated, was the possible absorption of significant amounts of RF energy at the cyclotron resonance of the minority species.

It is well known that in a two species plasma, the fast wave is heavily damped at the cyclotron resonance of the minority species¹⁶. If we were to allow the spatial

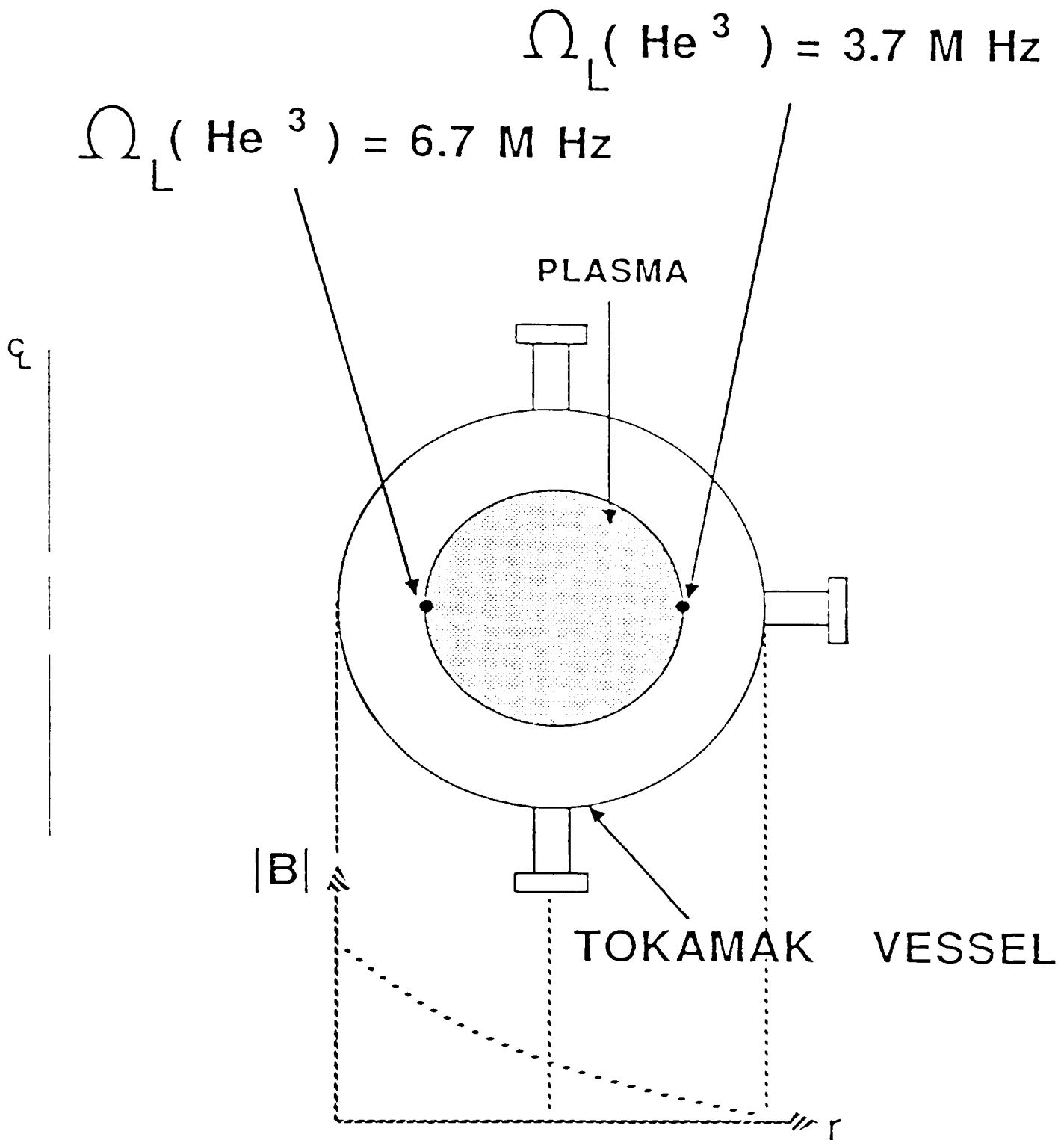


Fig. 2 Cross Section of Tokamak. Showing Value of the Cyclotron Resonance Frequency for He^3 at Plasma Edges.

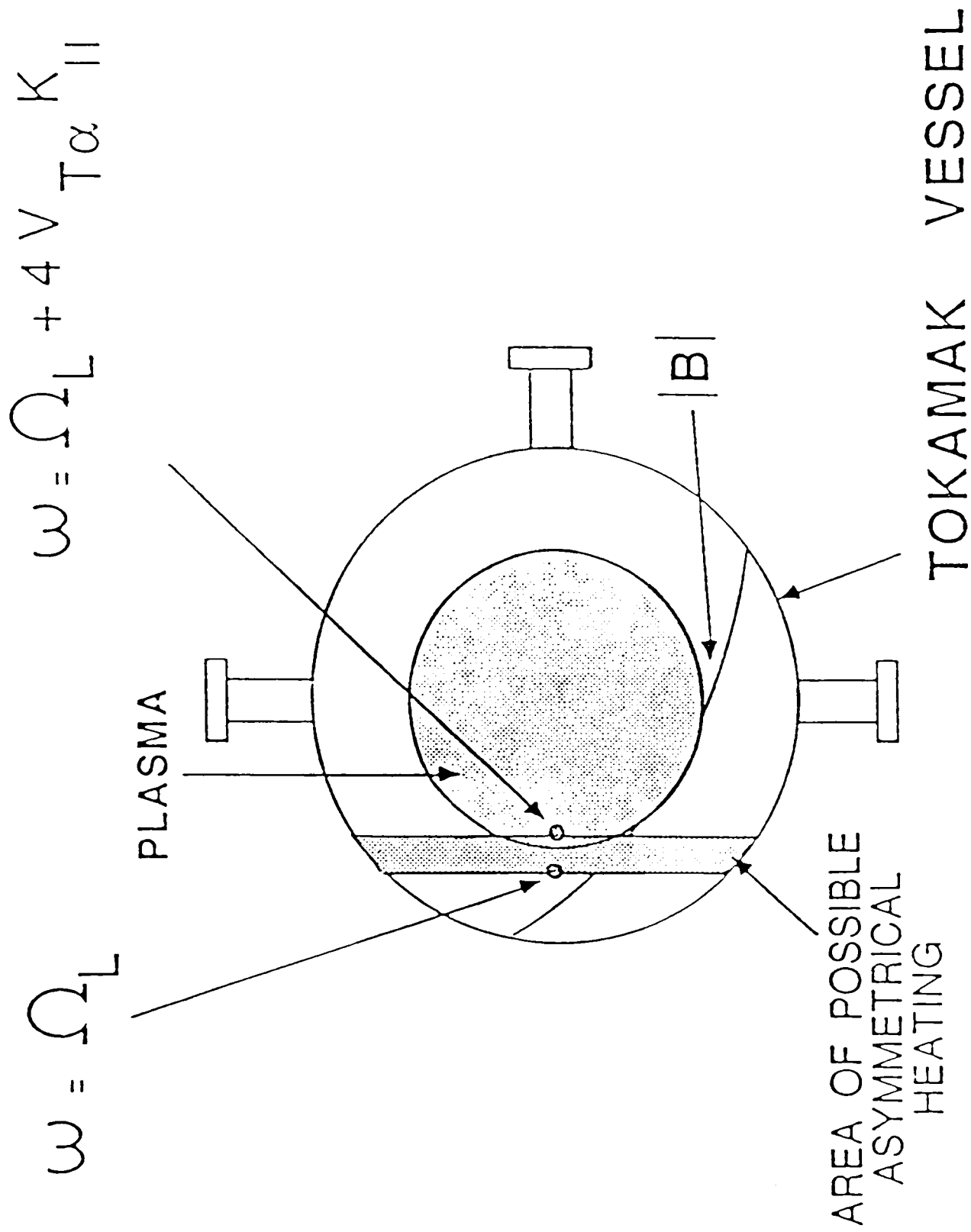


Fig. 3 Cross Section of Tokamak, Showing Area of Asymmetrical Heating with Edge of Plasma Satisfying $\omega = \Omega_L + 4V T \alpha_{\parallel} K_{\parallel}$.

location, where $\omega = \Omega_L$ is satisfied, to exist inside the plasma, instead of heating only minority ions with a certain parallel velocity, we would also heat the bulk ions, with the result of a greatly reduced amount of current drive being generated.

Unfortunately, our original plan, in practice, is impossible to carry out. In the Texas Tech Tokamak, the term $4V_{T\alpha}k_{\parallel}$ (using values for k_{\parallel} and $V_{T\alpha}$ experimentally obtained¹⁰) is much smaller than Ω_L . In fact, the spatial location which satisfies $\omega = \Omega_L$ and the spatial location which satisfies $\omega = \Omega_L + 4V_{T\alpha}k_{\parallel}$ are separated by less than two centimeters.

The plasma at the edge of our machine's plasma column is undoubtedly colder than the plasma at the center of its plasma column. In fact, the plasma at the edge is too cold (too collisional) to enable minority species heating. The question then becomes, "where is the plasma warm enough to support ion heating?" One could guess one-half or one centimeter into the plasma column but we do not have sufficient, space resolved temperature diagnostics to ascertain this. This location also most probably varies from one tokamak discharge to another. Beyond this, the magnetic field of the tokamak also varies slightly from shot to shot, varying the location of the heating layer, and making the prediction of its exact location difficult.

These difficulties, from a practical, experimental point of view, make it virtually impossible to place the asymmetrical heating layer, which corresponds to $\omega = \Omega_L + 4V_{T\alpha} k_{\parallel}$, inside the plasma column, where heating is possible, while at the same time, less than two centimeters away, placing the damping layer, which corresponds to $\omega = \Omega_L$, outside the plasma column. Even if we were able to place our current generating layer just at the edge of our plasma column, since the Texas Tech Tokamak's plasma is a rather cold tokamak plasma, most of the ions participating in current drive, being near the edge, would rapidly scatter out of the column, drastically reducing the current drive efficiency.

Unfortunately, our original plan to demonstrate current generation exactly as Fisch described it, was our only conceivable plan to do so. It appeared that the effect, exactly as Fisch described it, was impossible to demonstrate on the Texas Tech Tokamak. What we needed was a variation of the scheme, which was demonstrable on our tokamak.

Current Drive by Asymmetrical Heating of a One Ion Species Plasma

The current generation scheme that was ultimately investigated experimentally in the Texas Tech Tokamak was very similar to Fisch's original scheme, but differed in that only one species of ion, hydrogen, was used¹⁷. An

explanation of this effect can be given in terms of Fisch's original scheme.

As already mentioned, the effective charge of a hydrogenic tokamak plasma is $Z_{\text{eff}} \geq 2$ for virtually all existing tokamaks, including the Texas Tech Tokamak. Even for a one-species, hydrogen plasma, where there has been no intentional addition of a minority species, contaminants from the vessel's walls and limiters act to increase the effective charge of the tokamak plasma to $Z_{\text{eff}} \geq 2$. The essential idea in this new scheme is to use this fact to experimental advantage. Within the new scheme minority species ions are never intentionally added. All experiments were conducted with a one-species, hydrogen plasma, with an effective charge of $Z_{\text{eff}} \geq 2$.

If a unidirectional fast Alfvén wave were launched in the Texas Tech Tokamak with a frequency chosen to heat hydrogen ions moving in one particular direction around the torus, this heating would occur within a small portion of velocity space. Due to the variation in the toroidal magnetic field from the high field side of the machine to the low field side of the machine, this asymmetrical heating would occur within a small cross-sectional area in the machine (see Fig. 4). Hydrogen ions within this small area, streaming with the wave, would become hotter and hence collide less frequently with the background plasma than hydrogen ions streaming in the opposite direction within

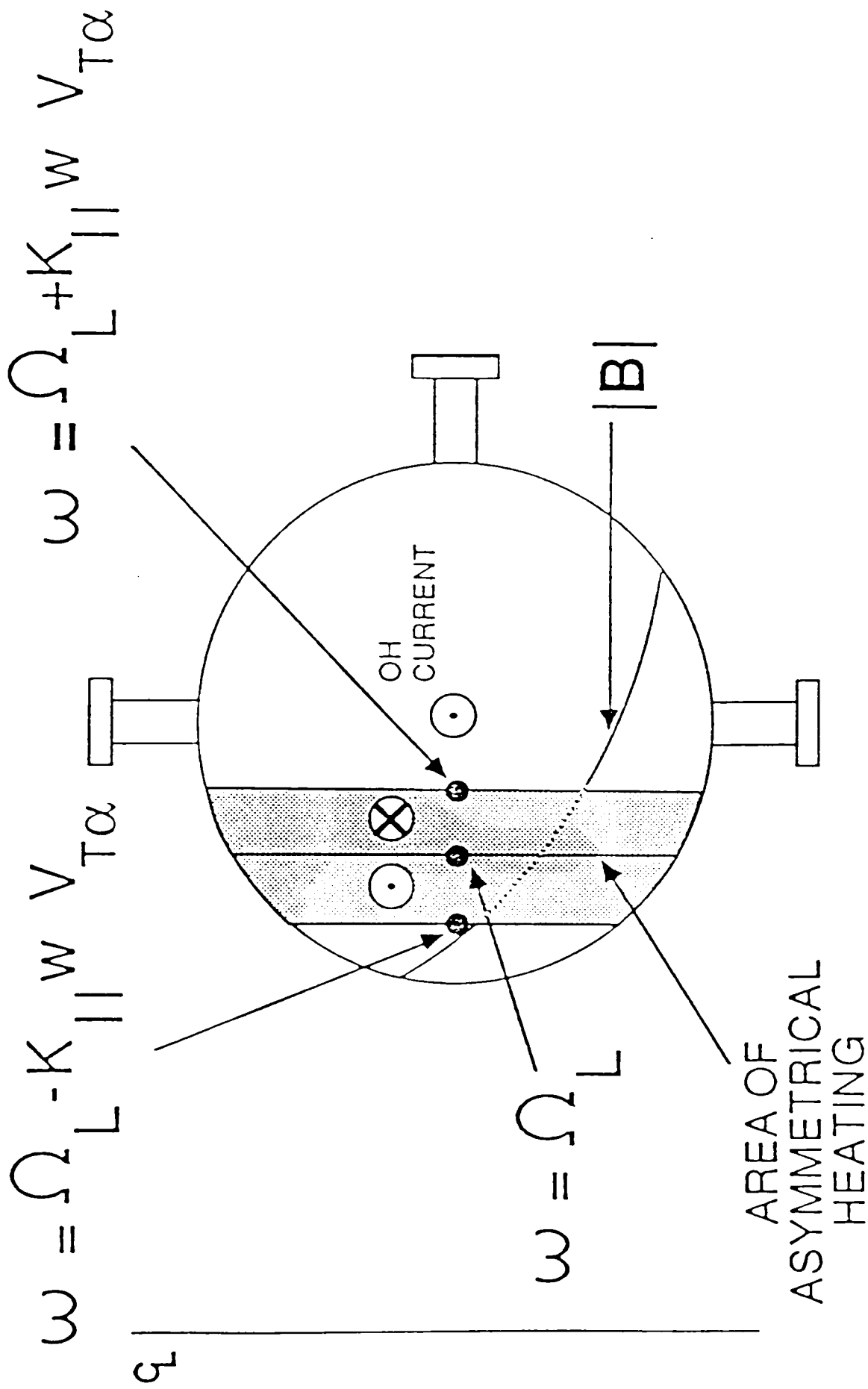


Fig. 4 Cross Section of Tokamak, Showing Area of Asymmetrical Heating. Particles Satisfying $\omega = \Omega_L + k_{||} W V_{Th}$ are Moving into the Page, Particles Satisfying $\omega = \Omega_L - k_{||} W V_{Th}$ are Moving out of the Page.

this small heating area. The background plasma is defined here as all hydrogen ions outside the small heating area and all impurities throughout the machine. In other words, all particles within the machine that are incapable of being heated by the Alfvén wave are considered to be part of the background plasma, which because of the influence of the impurities, has an effective charge of $Z_{\text{eff}} \geq 2$.

In terms of Fisch's original scheme, the hydrogen ions ($Z = 1$) within the area of possible asymmetrical heating could be called the "Fisch minority species" and the background plasma with $Z_{\text{eff}} \geq 2$ could be called the "Fisch majority species." During asymmetrical heating, hydrogen ions with charge $Z = 1$ would stream relative to the background plasma. Since the "Fisch minority species" has a different charge state than the "Fisch majority species," a toroidal current would result, in exactly the same manner as in Fisch's original scheme. Electrons would collide more frequently with the species having a larger electric charge, causing the electrons to experience a net ion drag and hence drift and produce a net current.

Current drive by the asymmetrical heating of a one-species plasma is similar to Fisch's original scheme in that current generation is localized within the tokamak. As in his scheme, asymmetrical heating only occurs for particles which satisfy

$$\omega = \Omega_L + k_{\parallel} W V_{T\alpha} \quad (29)$$

where Ω_L is again the local value of the "minority" ion cyclotron frequency, remembering now that the "minority" ion is hydrogen. As before, ω is the frequency of the RF power applied, k_{\parallel} is the parallel wave number of the fast Alfvén wave launched, and $W V_{T\alpha}$ is some multiple of the minority ion thermal velocity (typically $W \leq 4$)¹¹, where the "minority" ion, is again, hydrogen.

In the Texas Tech Tokamak, the term $4V_{T\alpha} k_{\parallel}$ (values of $V_{T\alpha}$ and k_{\parallel} found experimentally)¹⁰ is much smaller than the term Ω_L (the local cyclotron frequency for hydrogen, Ω_L , ranges from 5.6MHz to 10 MHz in our machine). In fact, it can be shown that the spatial location which satisfies $\omega = \Omega_L$ and the spatial location which satisfies $\omega = \Omega_L + 4V_{T\alpha} k_{\parallel}$ differ by only two centimeters or less in this tokamak. Thus all asymmetrical heating in the tokamak occurs in a small portion of the machine near the location which satisfies the condition $\omega = \Omega_L$.

It is now no longer a concern for us that the spatial location that satisfies $\omega = \Omega_L$ is within the plasma column. The reason for this is that in a hydrogen plasma (with or without heavy impurities from the tokamak vessel) which has no added minority species, there is no known damping mechanism of the fast Alfvén wave at the fundamental hydrogen cyclotron resonance. In fact, using cold plasma

theory, Stix predicts that the fast Alfvén wave in such a hydrogen plasma has no resonance at the hydrogen fundamental cyclotron frequency¹⁸.

However, it was of concern that perhaps the fast Alfvén wave could propagate at frequencies very near the fundamental hydrogen cyclotron frequency, a situation not ruled out by Stix's cold plasma calculations. If this were indeed the case, the Alfvén wave would be able to heat slow moving hydrogen ions, ions with low values of W . Large amounts of RF energy would go to heat these slow moving ions since there are many more of them than of fast moving ions. Since, as was already mentioned, slow moving ions convert RF energy to current drive less efficiently than fast moving ions, the resulting current drive efficiency would be very low indeed.

Since Stix predicts no resonance at the fundamental cyclotron frequency for the fast Alfvén in a hydrogen plasma using cold plasma theory¹⁸, it seemed possible that if the dispersion relation were calculated for the fast Alfvén wave in a hydrogen plasma, near the fundamental cyclotron frequency of hydrogen, using warm plasma theory^{19,20}, the dispersion relation would show that the fast wave could not damp near the fundamental hydrogen cyclotron frequency and therefore could not heat slow ions. The calculation of the dispersion relation of the fast Alfvén wave in a hydrogen plasma near the hydrogen cyclotron frequency is given in the

next section of this chapter. The result in short is that the assumption proved to be correct.

As mentioned previously, the term $4V_{T\alpha}k_{\parallel}$ is small compared to the term Ω_L . A consequence of this is that, for a given applied frequency, ω , the spatial locations which correspond to $\omega = \Omega_L + 4V_{T\alpha}k_{\parallel}$ and $\omega = \Omega_L - 4V_{T\alpha}k_{\parallel}$ are both likely to be in the plasma column. Of course, particles satisfying $\omega = \Omega_L + 4V_{T\alpha}k_{\parallel}$ are moving in the opposite direction to those satisfying $\omega = \Omega_L - 4V_{T\alpha}k_{\parallel}$. Therefore, especially in the case of a small tokamak (which possesses a lower plasma temperature and hence a lower value of $V_{T\alpha}$ than a large tokamak), the scheme of current drive by asymmetrical heating of a one-species plasma, generates two opposing layers of current generation (see Fig. 4).

This circumstance, at first glance, would seem to make experimental verification of current drive by asymmetrical heating of a one-species plasma difficult, if not impossible. However, there is, luckily, a quality inherent to small tokamaks which actually helps to facilitate confirmation of the effect. This effect, and the experimental procedure used to confirm current drive is explained in detail in Chapter 3.

If we assume that the background plasma (the "Fisch majority species") has an effective charge of exactly 2, or $Z_{\text{eff}} = 2$, and that the effective mass of the "Fisch majority species" is exactly one proton mass, or $m_i = m_{\alpha}$, a current

drive efficiency for this new, one-species current drive scheme can be derived. Using Eqs.(23), (25), and (28), and assuming that we heat only ions that are four times $V_{T\alpha}$ (or $W = 4$), we find an efficiency of approximately 30 milliamps of toroidal current for each watt of RF energy used. This value is comparable to the efficiency of Fisch's original scheme, corrected for temperature effects. Of course this value is much greater than the efficiency of his original scheme when corrected for $Z_{\text{eff}} \neq 1$, since if $Z_{\text{eff}} = 2$, the efficiency of his scheme goes to zero.

Dispersion Relation of the Fast Alfvén
Wave in a Hydrogen Plasma Near the
Fundamental Cyclotron Frequency

The following is a warm plasma calculation of the propagation of the fast Alfvén wave in a one-species, hydrogen plasma, near the fundamental cyclotron resonance of hydrogen. The calculation, which uses theory as developed by Stix¹⁹, closely follows an earlier calculation by Cato²⁰, where the dispersion relation of the fast Alfvén wave near the first harmonic of the ion cyclotron frequency was calculated.

The difference between warm plasma theory and cold plasma theory is, of course, that in warm plasma theory the particles are considered to have some non-zero temperature, and thus some thermal velocity. The velocity of the particles in some system is given by a particular velocity

distribution function. When the system is subjected to the effects of electromagnetic fields, the velocity distribution function of the system can be perturbed. The perturbation of the velocity distribution function can be found from Boltzmann's equation in terms of the perturbing fields. With this perturbed velocity distribution, the current density can be calculated and then combined with Maxwell's equations to find the dispersion relation.

Of course, the purpose here is not to rederive Stix's work, but simply to use it for the present calculations. Consequently, only the results of Stix's work together with additional simplifying assumptions are presented.

On his way to calculating the perturbed velocity distribution function, Stix obtains, as an intermediate result, a dimensionless mobility tensor, \vec{M} , defined by

$$\begin{aligned} \langle \vec{v}(\eta) \rangle &= \iiint \vec{v} f_1^{(\eta)} dV_X dV_Y dV_Z \\ &= \frac{1}{B_0} \vec{M}(\eta) \cdot \vec{E} \end{aligned} \quad (30)$$

where $\vec{v}(\eta)$ is a velocity vector for plasma particles of type η , B_0 is the static confining magnetic flux density, \vec{E} is the electric field, and $f_1^{(\eta)}$ is the first-order velocity distribution function for plasma particles of type η . The

matrix elements of \vec{M} will be given shortly. From the average velocities given by Eq.(30), the current density, \vec{J} , can be found as

$$\vec{J} = \sum_{\eta} N_{\eta} Z_{\eta} e \epsilon_{\eta} \langle \vec{v}^{(\eta)} \rangle, \quad (31)$$

where N_{η} is the zero-order density of particles of type η , Z_{η} is the absolute value of the charge of a particle of type η divided by e , e is 1.6×10^{-19} Coulombs, and ϵ_{η} equals +1 for ions, -1 for electrons.

In terms of the mobility tensor

$$\vec{J} = \sum_{\eta} N_{\eta} Z_{\eta} e \epsilon_{\eta} \frac{\vec{M}^{(\eta)} \cdot \vec{E}}{B_0}. \quad (32)$$

Assuming that all perturbed field quantities vary as

$\exp j(\vec{k} \cdot \vec{r} - \omega t)$, Maxwell's equations become

$$(\vec{j}k) \times (\vec{B} / \mu_0) = \vec{J} - j\omega\epsilon_0 \vec{E} \quad (33)$$

$$\vec{k} \times \vec{E} = \omega \vec{B} \quad (34)$$

where μ_0 is the permeability of vacuum, ϵ_0 is the

permittivity of vacuum, and \vec{k} is the propagation vector.

Inserting Eq.(32) into Eq.(33) and eliminating \vec{B} between Eqs.(33) and (34) yields

$$\vec{k} \times (\vec{k} \times \vec{E}) + \frac{\omega^2}{c^2} \vec{K} \cdot \vec{E} = 0 \quad (35)$$

where

$$\vec{K} = \vec{I} + j \sum_{\eta} N_{\eta} Z_{\eta} e \epsilon_{\eta} \frac{\vec{M}(\eta)}{B_0 \omega \epsilon_0}$$

is the equivalent dielectric tensor,

and

$$\vec{K} = \vec{I} + j \sum_{\eta} \frac{\omega_{P\eta}^2 \epsilon_{\eta}}{\omega \Omega_{\eta}} \vec{M}(\eta) \quad (36)$$

where $\omega_{P\eta}$ is the plasma frequency of type η particles, Ω_{η}

is the cyclotron frequency of type η particles, and \vec{I} is the identity tensor.

Cato used $N = ck/\omega$, where $|N|$ is the refractive index, to simplify the dispersion relation (Eq.(35)) to

$$\vec{N} \times (\vec{N} \times \vec{E}) + \vec{K} \cdot \vec{E} = 0 \quad (37)$$

and made the assumption that the cartesian coordinate system was positioned such that $\vec{B}_0 = \hat{e}_z B_0$ and \vec{k} (or \vec{N}) lies in the x-z plane (i.e. $k_y = 0$). Equation (37) then becomes, in matrix form,

$$\begin{bmatrix} -N_z^2 + K_{xx} & K_{xy} & N_x N_z + K_{xz} \\ K_{yx} & -N_x^2 - N_z^2 + K_{yy} & K_{yz} \\ N_x N_z + K_{zx} & K_{zy} & -N_x^2 + K_{zz} \end{bmatrix} \begin{bmatrix} E_x \\ E_y \\ E_z \end{bmatrix} = 0 \quad (38)$$

The desired dispersion relation is found by equating the determinant of the coefficient matrix to zero.

Now what is left is the definition of the mobility tensor. In the same cartesian coordinate system as just described, the mobility tensor components are defined in Eq.(39) with associated quantities (involving the averaging of velocity components over zero-order velocity distribution functions) described in Eq.(40).

$$M_{xx} = \frac{-\Omega \epsilon e^{-\lambda} \kappa T_{\perp}}{m k_z} \sum_{n=-\infty}^{\infty} \frac{n^2}{\lambda} I_n(\lambda) \langle \theta \rangle_n$$

$$M_{xy} = \frac{-\Omega e^{-\lambda} \kappa T_{\perp}}{m k_z} \sum_{n=-\infty}^{\infty} jn (I_n(\lambda) - I'_n(\lambda)) \langle \theta \rangle_n$$

$$\begin{aligned}
M_{xz} &= \frac{-\epsilon e^{-\lambda} \kappa T_{\perp}}{m k_z} \sum_{n=-\infty}^{\infty} \frac{n k_x}{\lambda} I_n(\lambda) (n \langle \phi \rangle_n - \langle \psi \rangle_n) \\
M_{yx} &= \frac{-\Omega e^{-\lambda} \kappa T_{\perp}}{m k_z} \sum_{n=-\infty}^{\infty} -j n (I_n(\lambda) - I'_n(\lambda)) \langle \theta \rangle_n \\
M_{yy} &= \frac{-\Omega \epsilon e^{-\lambda} \kappa T_{\perp}}{m k_z} \sum_{n=-\infty}^{\infty} \left(\frac{n^2}{\lambda} I_n(\lambda) + 2\lambda I_n(\lambda) \right. \\
&\quad \left. - 2\lambda I'_n(\lambda) \right) \langle \theta \rangle_n \\
M_{yz} &= \frac{-e^{-\lambda} \kappa T_{\perp}}{m k_z} \sum_{n=-\infty}^{\infty} -j k_x (I_n(\lambda) - I'_n(\lambda)) (n \langle \phi \rangle_n - \langle \psi \rangle_n) \\
M_{zx} &= \frac{-e^{-\lambda} \kappa \epsilon T_{\perp}}{m k_z} \sum_{n=-\infty}^{\infty} \frac{-n k_x}{\lambda} I_n(\lambda) \langle v_z \theta \rangle_n \\
M_{zy} &= \frac{-e^{-\lambda} \kappa T_{\perp}}{m k_z} \sum_{n=-\infty}^{\infty} -j k_x (I_n(\lambda) - I'_n(\lambda)) \langle v_z \theta \rangle_n \\
M_{zz} &= \frac{\Omega \epsilon e^{-\lambda}}{k_z} \sum_{n=-\infty}^{\infty} I_n(\lambda) (n \langle v_z \phi \rangle_n - \langle v_z \psi \rangle_n),
\end{aligned} \tag{39}$$

where $\lambda = \frac{k_x^2 \kappa T_{\perp}}{\Omega_{\eta}^2 m_{\eta}}$, k_x is the wave number perpendicular to \vec{B}_0 , $k_z = k_{\parallel}$ is the wave number parallel to \vec{B}_0 , κ is the Boltzmann constant, T_{\perp} is the perpendicular temperature, m_{η}

is the mass of a particle of type η , and $I_n(\lambda)$ is the modified Bessel function of n^{th} order.

$$\begin{aligned}
\langle \theta \rangle_n &= \frac{2}{T_{\perp} v_{\parallel}^3 \omega} \{ jk_z v_{\parallel} (T_{\perp} - T_{\parallel}) \\
&\quad - [(\omega - k_z V_z + n\Omega) T_{\perp} - n\Omega T_{\parallel}] F_0(\alpha_n) \} \\
\langle \phi \rangle_n &= \frac{2\Omega}{k_z T_{\perp} v_{\parallel}^3 \omega} \{ jk_z v_{\parallel} (T_{\perp} - T_{\parallel}) \\
&\quad + [(\omega - k_z V_z + n\Omega) T_{\perp} - (\omega + n\Omega) T_{\parallel}] F_0(\alpha_n) \} \\
\langle \psi \rangle_n &= \frac{2}{k_z v_{\parallel}^3} \{ jk_z v_{\parallel} - (\omega - k_z V_z + n\Omega) F_0(\alpha_n) \} \\
\langle v_z \theta \rangle_n &= \frac{2}{k_z T_{\perp} v_{\parallel}^3 \omega} \{ jk_z v_{\parallel} [(\omega + n\Omega) T_{\perp} - (k_z V_z + n\Omega) T_{\parallel}] \\
&\quad - (\omega + n\Omega) [(\omega - k_z V_z + n\Omega) T_{\perp} - n\Omega T_{\parallel}] F_0(\alpha_n) \} \\
\langle v_z \phi \rangle_n &= \frac{2\Omega}{k_z^2 T_{\perp} v_{\parallel}^3 \omega} \{ jk_z v_{\parallel} [(-\omega - n\Omega) T_{\perp} + (\omega + k_z V_z \\
&\quad + n\Omega) T_{\parallel}] + (\omega + n\Omega) [(\omega - k_z V_z + n\Omega) T_{\perp} \\
&\quad - (\omega + n\Omega) T_{\parallel}] F_0(\alpha_n) \} \\
\langle v_z \psi \rangle_n &= \frac{2}{k_z^2 v_{\parallel}^3} \{ jk_z v_{\parallel} (\omega + n\Omega) \\
&\quad - (\omega + n\Omega) (\omega - k_z V_z + n\Omega) F_0(\alpha_n) \} .
\end{aligned} \tag{40}$$

where

$$F_0(\alpha_n) = \sqrt{\pi} \frac{k_z}{|k_z|} e^{-(\alpha_n)^2} + 2j e^{-(\alpha_n)^2} \int_0^{\alpha_n} e^{t^2} dt ,$$

$$\alpha_n = \frac{\omega - k_z V_z + n\Omega}{k_z v_{\parallel}} ,$$

$$v_{\parallel} = \left[\frac{2\kappa T_{\parallel}}{m} \right]^{1/2} ,$$

T_{\parallel} is the parallel temperature, and V_z is the parallel drift velocity.

From Eq.(39) it is obvious that $M_{xy} = -M_{yx}$. From Eq.(40) we can also note that

$$n\langle\phi\rangle_n - \langle\psi\rangle_n = -\langle v_z \theta \rangle - \frac{jk_z v_z}{\omega} \left[\frac{m}{\kappa T_{\parallel}} \right]$$

which, when used with the Bessel function identities for integral n , $I_n(\lambda) = I_{-n}(\lambda)$ and $\sum_{n=-\infty}^{\infty} (I_n(\lambda) - I_{-n}(\lambda)) = 0$, can be used to show that $M_{xz} = M_{zx}$ and $M_{yz} = -M_{zy}$. There are \Rightarrow thus only six independent terms in M , but it is obvious from Eqs.(39) and (40) that evaluating even just six terms is going to be rather difficult. Consequently, we would like to simplify the remaining mobility tensor terms in any reasonable way.

If we recall the power series representation of $I_n(\lambda)$

$$I_n(\lambda) = \sum_{v=0}^{\infty} \frac{\left[\frac{\lambda}{2} \right]^{2v+n}}{v! (n+v)!} \quad (41)$$

and use it in M_{xx} and recall the fact that $I_n(\lambda) = I_{-n}(\lambda)$ for integral n , we find

$$M_{xx} = \frac{-\Omega \epsilon \kappa T_{\perp}}{m k_z} e^{-\lambda} \sum_{n=1}^{\infty} \sum_{v=0}^{\infty} \frac{n^2}{2} \frac{\left[\frac{\lambda}{2} \right]^{2v+n-1}}{v! (n+v)!} [\langle \theta \rangle_n - \langle \theta \rangle_{-n}]. \quad (42)$$

To reduce algebraic complexity, we assume that the plasma is only "moderately hot" (which is a fair approximation in our

case), or that $\lambda \ll 1$ (recalling that $\lambda = \frac{k_x^2 \kappa T_{\perp}}{\Omega_{\eta}^2 m_{\eta}}$). In

this approximation, the terms of M_{xx} up to the first order in λ of the power series give a fair approximation to M_{xx} .

Using $e^{-\lambda} \cong 1 - \lambda$ and power series expressions like the one found for the term M_{xx} , the mobility terms, correct up to the first-order in λ , can be given as

$$M_{xx} \approx \frac{-\Omega \epsilon \kappa T_{\perp}}{2m k_z} [\langle \theta \rangle_1 (1 - \lambda) + \langle \theta \rangle_{-1} (1 - \lambda) + \lambda \langle \theta \rangle_2 + \lambda \langle \theta \rangle_{-2}]$$

$$\begin{aligned}
M_{xy} = -M_{yx} &\approx \frac{j\Omega\kappa T_{\perp}}{2mk_z} [\langle\theta\rangle_1(1-2\lambda) - \langle\theta\rangle_{-1}(1-2\lambda) + \lambda\langle\theta\rangle_2 \\
&\quad - \lambda\langle\theta\rangle_{-2}] \\
M_{xz} = M_{zx} &\approx \frac{-k_x\epsilon\kappa T_{\perp}}{2mk_z} [\langle v_z\theta\rangle_1(1-\lambda) - \langle v_z\theta\rangle_{-1}(1-\lambda) \\
&\quad + \frac{\lambda}{2}\langle v_z\theta\rangle_2 - \frac{\lambda}{2}\langle v_z\theta\rangle_{-2}] \\
M_{yy} &\approx \frac{-\Omega\epsilon\kappa T_{\perp}}{2mk_z} [\langle\theta\rangle_1(1-3\lambda) + \langle\theta\rangle_{-1}(1-3\lambda) + 4\langle\theta\rangle_0 + \lambda\langle\theta\rangle_2 \\
&\quad + \lambda\langle\theta\rangle_{-2}] \\
M_{yz} = -M_{zy} &\approx \frac{-jk_x\kappa T_{\perp}}{2mk_z} [\langle v_z\theta\rangle_0(2-3\lambda) - \langle v_z\theta\rangle_1(1-2\lambda) \\
&\quad - \langle v_z\theta\rangle_{-1}(1-2\lambda) - \frac{\lambda}{2}\langle v_z\theta\rangle_2 - \frac{\lambda}{2}\langle v_z\theta\rangle_{-2}] \\
M_{zz} &\approx \frac{-\Omega\epsilon}{2k_z} [2\langle v_z\psi\rangle_0(1-\lambda) - \lambda\langle v_z\phi\rangle_1 + \lambda\langle v_z\psi\rangle_1 + \lambda\langle v_z\phi\rangle_{-1} \\
&\quad + \lambda\langle v_z\psi\rangle_{-1}].
\end{aligned} \tag{43}$$

To simplify the quantities of Eq.(40), in addition to assuming λ small, we assume that $T_{\perp} = T_{\parallel} = T$, and that the plasma drift velocity V_z , equals zero. These assumptions simplify the quantities in Eq.(40) considerably:

$$\langle\phi\rangle_n = \langle v_z\phi\rangle_n = 0$$

$$\langle \psi \rangle_n = \langle v_z \theta \rangle_n = \frac{2j}{v_{\parallel}^2} - \frac{2(\omega + n\Omega) F_o(\alpha_n)}{k_z v_{\parallel}^3}$$

$$\langle \theta \rangle_n = \frac{-2 F_o(\alpha_n)}{v_{\parallel}^3}$$

$$\langle v_z \psi \rangle_n = \frac{2j(\omega + n\Omega)}{k_z v_{\parallel}^2} - \frac{2(\omega + n\Omega)^2 F_o(\alpha_n)}{k_z^2 v_{\parallel}^3} .$$

When these values are substituted into Eq.(43), the simplified mobility tensor elements become

$$M_{xx} \approx \frac{-\Omega \epsilon \kappa T}{2mk_z} \left[\frac{-2}{v_{\parallel}^3} \{ F_o(\alpha_1) - F_o(\alpha_{-1}) + \lambda (F_o(\alpha_2) + F_o(\alpha_{-2})) \} \right]$$

$$M_{xy} = -M_{yx} \approx \frac{j\Omega \kappa T}{2mk_z} \left[\frac{-2}{v_{\parallel}^3} \{ F_o(\alpha_1) - F_o(\alpha_{-1}) + \lambda (F_o(\alpha_2) - F_o(\alpha_{-2})) \} \right]$$

$$M_{yy} \approx \frac{-\Omega \epsilon \kappa T}{2mk_z} \left[\frac{-2}{v_{\parallel}^3} \{ F_o(\alpha_1) + F_o(\alpha_{-1}) + 4\lambda F_o(\alpha_0) + \lambda (F_o(\alpha_2) + F_o(\alpha_{-2})) \} \right]$$

$$M_{zz} \approx \frac{-\Omega\epsilon}{2k_z} \left[\frac{4j\omega}{k_z v_{\parallel}^3} - \frac{1}{k_z^2 v_{\parallel}^3} \{ 4\omega^2 F_0(\alpha_0) \right. \\ \left. + \lambda (2(\omega + \Omega)^2 F_0(\alpha_1) + 2(\omega - \Omega)^2 F_0(\alpha_{-1})) \} \right]$$

$$M_{xz} = M_{zx} \approx \frac{-k_x \epsilon \kappa T}{2mk_z^2 v_{\parallel}^3} \{ -2(\omega + \Omega)F_0(\alpha_1) + 2(\omega - \Omega)F_0(\alpha_{-1}) \\ + \lambda [-(\omega + 2\Omega)F_0(\alpha_2) + (\omega - 2\Omega)F_0(\alpha_{-2})] \}$$

$$M_{yz} = -M_{zy} \approx \frac{-k_x \kappa \lambda T}{mk_z v_{\parallel}^2} + \frac{-jk_x \kappa T}{2mk_z^3 v_{\parallel}^3} \{ -4\omega F_0(\alpha_0) \\ + 2(\omega + \Omega)F_0(\alpha_1) + 2(\omega - \Omega)F_0(\alpha_{-1}) \\ + \lambda [(\omega + 2\Omega)F_0(\alpha_2) + (\omega - 2\Omega)F_0(\alpha_{-2})] \}$$

Now to find the elements of the equivalent dielectric

tensor, \vec{K} , we need to make use of Eq.(36)

$$\vec{K} = \vec{I} + j \sum_{\eta} \frac{\omega_{p\eta}^2 \epsilon_{\eta}}{\omega - \Omega_{\eta}} \vec{M}(\eta). \quad (36)$$

Since we are trying to find the dispersion relation of the fast wave in a hydrogen plasma, and since η refers to a "type" of particle, we need only to sum over electrons and protons to find the dispersion relation.

However, there is one last thing to define in the mobility tensor before one can find the dispersion relation.

and that is the various values of the function $F_o(\alpha_n)$. With the assumption $V_z = 0$, α_n for protons becomes

$$\alpha_{ni} = \frac{\omega + n\Omega_i}{k_z v_{\parallel i}} \quad (46)$$

and for electrons

$$\alpha_{ne} = \frac{\omega + n\Omega_e}{k_z v_{\parallel e}} \quad (47)$$

where Ω_i is the cyclotron frequency for protons, Ω_e is the cyclotron frequency for electrons, $v_{\parallel i}$ is the parallel thermal velocity of the protons and $v_{\parallel e}$ is the parallel thermal velocity of the electrons.

In an attempt to solve the dispersion relation near the ion cyclotron resonance of hydrogen ($\omega \approx \Omega_i$), we assumed that $|\alpha_n| \gg 1$ ($n \neq -1$). Stix tells us¹⁹, that for $|\alpha_n| \gg 1$, $F_o(\alpha_n) \approx j/\alpha_n$. Therefore, the only values of the function $F_o(\alpha_n)$ that must be found are for the case when $n = -1$ for protons, or $F_o\left[\frac{\omega - \Omega_i}{k_z v_{\parallel i}}\right]$, which we will be denoted from now on as $F_o(\alpha_{-1})$.

The function $F_o(x)$ is known in terms of a better known function, the Z function, as

$$F_o(x) = -j Z(x) \quad (48)$$

where x is a real number. We can therefore insert the proper value of $F_0(\alpha_{-1})$ into the calculation, as parameters vary, by using values of the Z function, tabulated by Fried and Conte²¹.

We are now ready to state the elements of the equivalent dielectric tensor as

$$\begin{aligned}
 K_{xx} = K_{yy} = K_1 &= 1 - \frac{\omega_{pe}^2}{2\omega(\omega + \Omega_e)} - \frac{\omega_{pe}^2}{2\omega(\omega - \Omega_e)} \\
 &\quad - \frac{\omega_{pi}^2}{2\omega(\omega + \Omega_i)} - \frac{\omega_{pi}^2 F_0(\alpha_{-1})}{2j\omega k_z v_{\parallel i}} \\
 K_{xy} = -K_{yx} = K_2 &= \frac{j\omega_{pi}^2}{2\omega(\omega + \Omega_i)} - \frac{\omega_{pi}^2 F_0(\alpha_{-1})}{2\omega k_z v_{\parallel i}} \\
 &\quad - \frac{j\omega_{pe}^2}{2\omega(\omega + \Omega_e)} + \frac{j\omega_{pe}^2}{2\omega(\omega - \Omega_e)}
 \end{aligned}
 \tag{49}$$

$$K_{zz} = K_3 = 1 + \frac{-k_x \omega_{pe}^2}{k_z^2 \Omega_e^2} + \frac{-k_x \omega_{pi}^2}{2k_z^2 \Omega_i^2 \omega} \left[\omega + \Omega_i + \frac{(\omega - \Omega_i)^2 F_0(\alpha_{-1})}{jk_z v_{\parallel i}} \right]$$

$$K_{xz} = K_{zx} = K_4 = \frac{\omega_{pi}^2 k_x}{2\Omega_i k_z \omega} \left[\frac{(\omega - \Omega_i) F_0(\alpha_{-1})}{jk_z v_{\parallel i}} - 1 \right]$$

$$K_{yz} = -K_{zy} = K_5 = \frac{-\omega_{pe}^2 k_x^3 v_{\parallel e}^2 (1 + (1/k_z))}{4\omega\Omega_e^2 k_z} + \frac{\omega_{pi}^2 k_x^2}{2\omega\Omega_i k_z^2} \left[\frac{(\omega - \Omega_i) F_0(\alpha_{-1})}{jk_z v_{\parallel i}} - 1 \right].$$

Now recalling the coordinate system, one can label the angle between \vec{B}_0 and \vec{k} (or \vec{N}) as θ , which allows one to write $N_z = N \cos(\theta)$ and $N_x = N \sin(\theta)$. With these relations and Eq.(49), one can rewrite Eq.(38) as

$$\begin{bmatrix} K_1 - N^2 \cos^2 \theta & K_2 & K_4 + N^2 \sin \theta \cos \theta \\ -K_2 & K_1 - N^2 & K_5 \\ K_4 + N^2 \sin \theta \cos \theta & -K_5 & K_3 - N^2 \sin^2 \theta \end{bmatrix} \begin{bmatrix} E_x \\ E_y \\ E_z \end{bmatrix} = 0. \quad (50)$$

By equating the determinant of the coefficient matrix to zero, one finds the desired dispersion relation as

$$\begin{aligned} & N^4 [K_1 \sin^2 \theta + K_3 \cos^2 \theta + 2K_4 \sin \theta \cos \theta] \\ & + N^2 [-\sin^2 \theta (K_1^2 + K_2^2) - K_1 K_3 (1 + \cos^2 \theta) + K_2 K_5 (2 \sin \theta \cos \theta) \\ & \quad + K_4^2 - K_5^2 \cos^2 \theta - 2K_1 K_4 \sin \theta \cos \theta] \\ & + [K_3 (K_1^2 + K_2^2) + K_1 (-K_4^2 + K_5^2) + K_2 K_4 K_5] = 0. \end{aligned} \quad (51)$$

Equation (51) can be solved numerically for N and ω (where $N = ck/\omega$), as a function of position within the

tokamak (or in other words, as a function of magnetic field, or in still other words, as a function of the local electron and ion cyclotron resonances). Values (such as the plasma frequencies, the parallel wave number, and the ion temperature) which are characteristic of the Texas Tech Tokamak were inserted into the elements of the dielectric tensor (characteristic parameters of the Texas Tech Tokamak are presented in Chapter 3). These values were considered constant, an approximation made for ease of calculation. Interestingly, the electron temperature (within a reasonable range of values) has no effect on the dispersion relation, which one might expect, since we assume that the principal physical phenomenon affecting the wave is its frequency's proximity to the ion cyclotron frequency.

What results after the insertion of constants in Eq.(51) is a function of the type

$$\omega_r + j\omega_i = f(\omega_r, r, k_x) \quad (52)$$

where ω_r and ω_i are respectively, of course, the real and imaginary parts of ω , k_x is the wave number in the x direction, and r refers to the radial location within the tokamak. Within the calculation, the frequency inserted into the function $f(\omega_r, r, k_x)$ was $\omega_r = 4.4 \times 10^7$ rad/sec, a frequency corresponding to the frequency of a fast Alfvén wave known to exist experimentally within the Texas Tech

Tokamak, and a frequency corresponding to a hydrogen ion cyclotron resonance, Ω_L , on the high field side of the tokamak (see Fig.5). Then for various locations within a few centimeters on either side of the spatial location where $\omega = \Omega_L = 4.4 \times 10^7$ rad/sec is satisfied, values of k_x were sought that would result in the two ω_r values in Eq.(52) converging. Once the two ω_r values had converged, the value of ω_i and hence the degree to which the fast wave was damped at that particular spatial location could be determined.

The results are illustrated graphically in Fig.5. For spatial locations which correspond to the heating of ions with velocities ± 6 or ± 7 times the thermal velocity ($\omega = \Omega_L \pm 6V_{T\alpha}k_{\parallel}$, $\omega = \Omega_L \pm 7V_{T\alpha}k_{\parallel}$) a value of k_x that would cause the two ω_r values to converge could easily be found. The resulting value of ω_i is extremely small (on the order of 10 rad/sec), which suggests that at these spatial locations, the wave propagates without significant damping (damping time is on the order of 100 msec) resulting in no heating of ions.

For spatial locations which correspond to the heating of ions with velocities ± 5 , ± 4 , or ± 3 times the thermal velocity ($\omega = \Omega_L \pm 5V_{T\alpha}k_{\parallel}$, $\omega = \Omega_L \pm 4V_{T\alpha}k_{\parallel}$, $\omega = \Omega_L \pm 3V_{T\alpha}k_{\parallel}$) again a value of k_x that would cause the two ω_r values to converge could again be found (though not as easily as before) but now the resulting value of ω_i had increased significantly (from one to several orders of

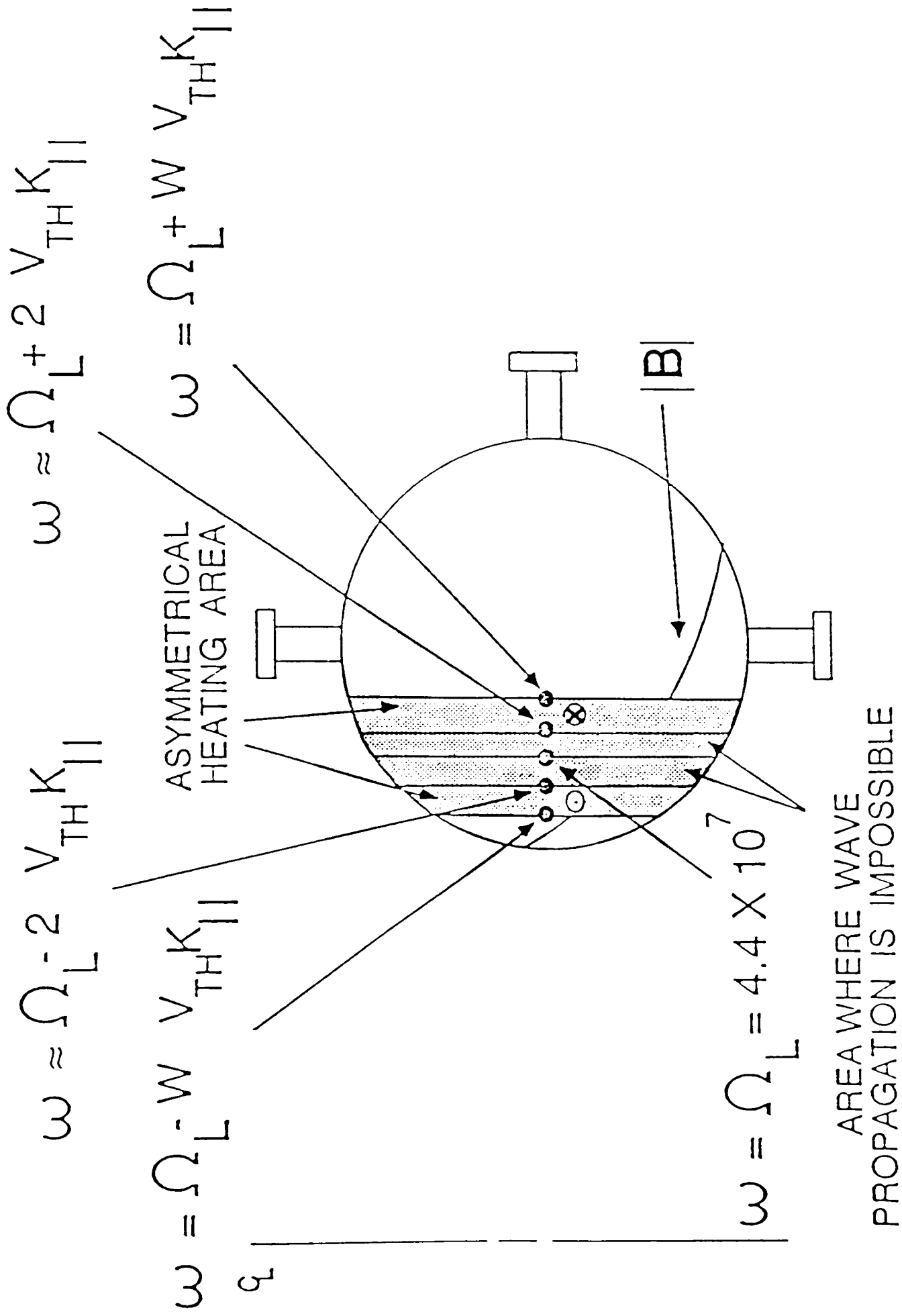


Fig. 5 Cross section of Tokamak, Showing Area of Asymmetrical Heating and Area Where Wave is Unable to Propagate.

magnitude larger). From this follows the conclusion that the wave still propagates in this area, but now damps, and thus heats ions.

For spatial locations which correspond to the heating of ions with velocities ± 2 , ± 1 , or zero times the thermal velocity ($\omega = \Omega_L \pm 2V_{T\alpha}k_{\parallel}$, $\omega = \Omega_L \pm V_{T\alpha}k_{\parallel}$, $\omega = \Omega_L$) no value of k_x that would cause the two ω_r values to converge could be found. In these locations therefore, the fast wave is cut off, unable to propagate.

It appears that not only is there no resonance at the hydrogen ion cyclotron resonance frequency, as Stix predicts¹⁹, but beyond this, the fast Alfvén wave cannot even propagate near the ion cyclotron resonance frequency. This fact, which prevents the heating of slow hydrogen ions (which are, as we have seen, inefficient for current generation), seems to make possible the demonstration of current generation by asymmetrical heating of a one-species plasma in the Texas Tech Tokamak.

CHAPTER III

EXPERIMENTAL APPARATUS AND PROCEDURE

Tokamak and Associated Equipment

The following is a short description of the Texas Tech Tokamak. This device has been described in various works^{11,22,23} and has been extensively documented by Kirbie²⁴.

The basic design of the Texas Tech Tokamak is not original, but a modification of several preceding circular cross section tokamaks with air-core, ohmic heating transformers. The first tokamak of this type in the United States was built at the Francis Bitter National Magnet Laboratory in the mid 1970's. A tokamak very similar to the Texas Tech Tokamak was built somewhat later by Professor R. M. Gould at the California Institute of Technology²⁶.

The Texas Tech Tokamak was designed to produce a plasma hot enough to enable studies of wave propagation and plasma heating with waves in the ion cyclotron range of frequencies. Extensive research on the fast Alfvén wave, in particular, has been carried out^{11,22,23,27,28,29}.

The following are short descriptions of various characteristics and parameters of the tokamak. Also included

are descriptions of various pieces of equipment associated with the machine.

Vacuum Chamber

A top view of the Texas Tech Tokamak's stainless steel vacuum vessel is shown in Fig. 6. The tokamak has 22 vacuum ports, with a total access area of 550 cm^2 .

Toroidal Field

The toroidal field coil, wound directly on the insulated metal chamber, is energized by a 2.56 mF capacitor bank. When the bank is charged to a typical voltage of 6 kV, a magnetic field of .5 T is produced at the poloidal axis of the machine.

Plasma Current

A 50 turn, ohmic heating, air-core winding drives a maximum plasma current of 15 kA. The winding is driven by a two stage capacitor bank with a fast bank of $980 \mu\text{F}$ at 3 kV and a slow bank of 100 mF at 600 V.

If no probes are inserted into the plasma, a current is driven and a plasma exists for a maximum of 10 ms. During the present experiments, a large antenna structure placed within the vacuum vessel undoubtedly injected impurities into the plasma. Most probably for this reason, a typical discharge during these experiments was approximately 1.5 ms.

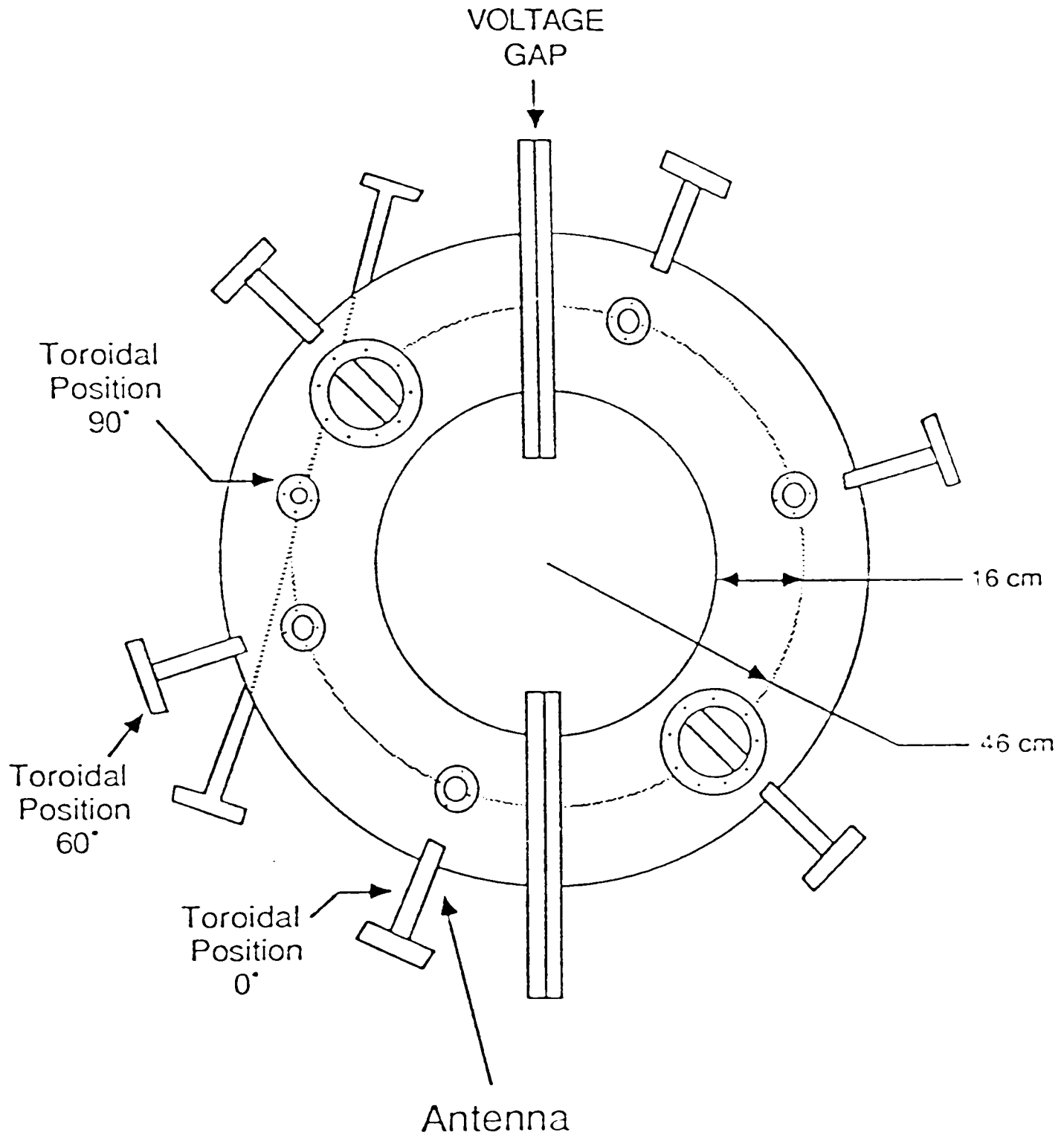


Fig. 6 Top View of Texas Tech Tokamak Vacuum Chamber.

Vertical Field

Radial plasma column motion, due primarily to the plasma's diamagnetic quality, can be controlled by an externally applied vertical magnetic field. A vertical field coil is wound inside the ohmic heating transformer of the Texas Tech Tokamak. The coil is energized by a two stage capacitor bank with a fast bank of 500 μF at 1 kV and a slow bank of 15.5 mF at 500 V (see Fig. 7).

Radial Field

A radial field coil, exterior to all other field coils on the Texas Tech Tokamak, forms a cusp field within the machine's vacuum chamber. Vertical plasma column motion, due to field errors, can be controlled by applying an external radial field. Since most of the vertical drift is caused by toroidal field imperfections, the applied radial field should follow the toroidal field in time. For this reason, the radial field coil is energized by sampling a controlled amount of the toroidal field winding's current.

Plasma Density

The Texas Tech Tokamak has a peak, line-averaged central electron density of $1.2 \times 10^{13} \text{ cm}^{-3}$. This density is measured by a 70 GHz microwave interferometer.

Plasma Temperature

The Texas Tech Tokamak has an electron temperature of approximately 100 eV and an ion temperature of approximately

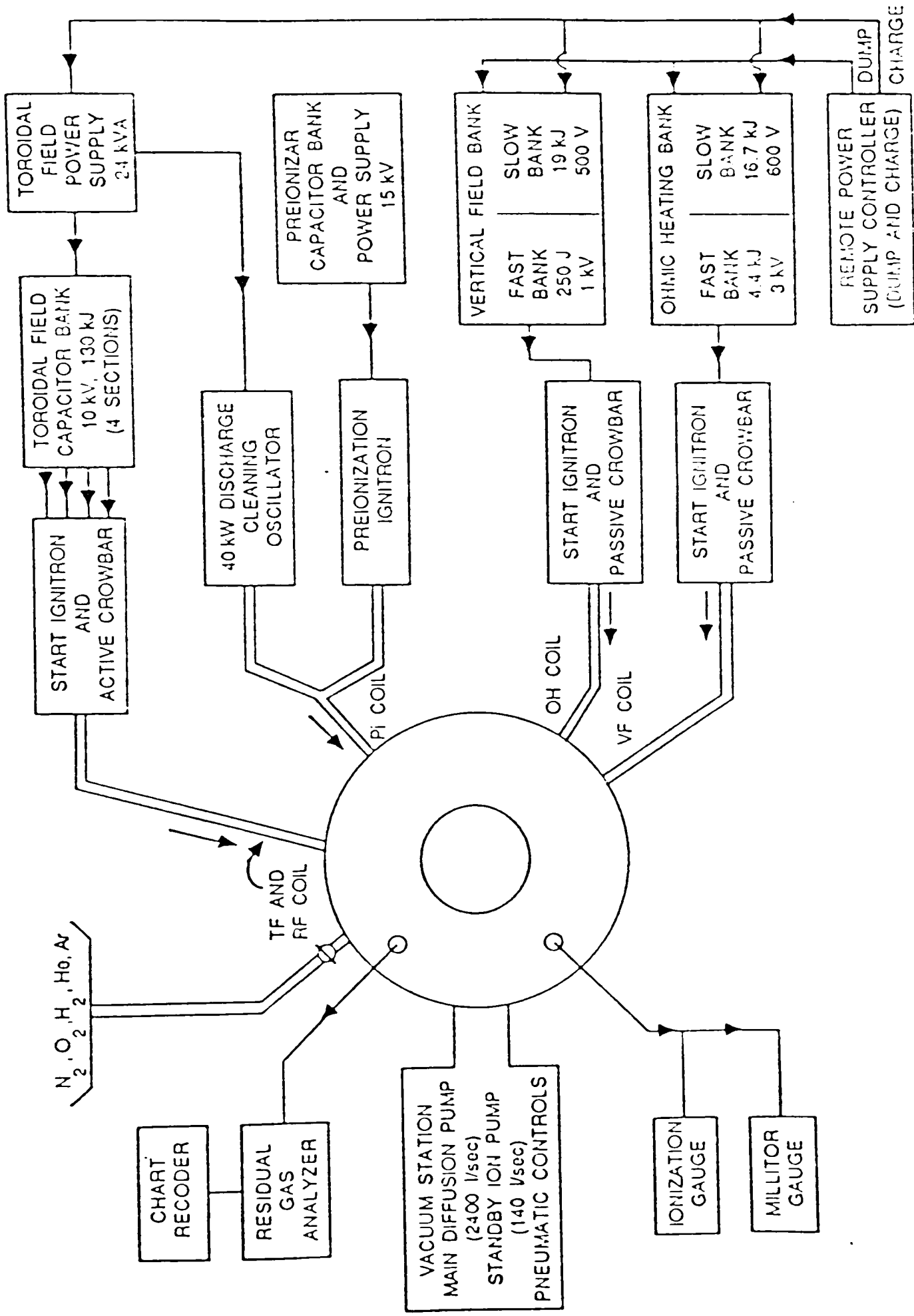


Fig. 7 Block Diagram of the Texas Tech Tokamak Facility.

20-40 eV. Ion temperature measurements were made with a monochromator by observing the Doppler-broadening of a HeII line. The electron temperature was estimated through Spitzer resistivity calculations by assuming $Z_{\text{eff}} = 2$.

Other Diagnostics

The toroidal field, ohmic heating, and vertical field excitation currents are monitored by self integrating current transformers. The machine's loop voltage is measured with 2 one-turn loops in the equatorial plane, next to the tokamak's vacuum chamber. The toroidal magnetic field and plasma current are measured with passively integrated Rogowski coils. The plasma column's position is determined by a sine coil for axial (up-down) movement, and a cosine coil for radial (in-out) motion. Toroidal eigenmodes of the fast Alfvén wave are detected by \dot{B} probes placed within the vacuum vessel at the plasma column's edge.

Slow Wave Antenna

Two slow wave antennas were used during the course of the research on current drive by asymmetrical heating of ions in the Texas Tech Tokamak. Of the two antennas (which differed in only a few minor respects) the original is very well documented^{23,30}, and is the major subject of the brief description that follows. The second antenna and how it differs from the original one are briefly discussed.

Antenna Structure

The original antenna is a short, rectangularly coiled, slow wave antenna. The slow wave nature of the antenna allows it to launch unidirectional Alfvén waves. The antenna consists of a copper coil lying on a 10" by 5.25" by 3/8" stainless steel tray that is enclosed by a stainless steel Faraday shield. The coil is wound from a 0.75" thick, .325" wide copper strip. The coil has 16 1/2 rectangular turns, each turn with inner dimensions of .375" by 3.300". The axial length of the coil is 6.60" (see Figs. 8 and 9).

The coil is insulated from its stainless steel tray by a thin sheet of teflon. The antenna is designed so that the distance between the coil and the tray can be varied slightly to change the capacitance of the coil and thus to fine tune the impedance of the antenna to match that of the transmission line feeding it. Thus, no matching circuitry between the antenna and the transmission line is necessary.

With no matching circuitry, the high reactive voltages associated with matching circuitry are eliminated. In this antenna system, a 30 kW RF pulse into 50 Ω results in a peak-to-peak voltage at the feed-throughs of only 3500 V. The same pulse in the matching circuitry of a loop antenna would produce approximately 15 kV at the feedthroughs. This approach therefore greatly simplifies the feed-through design.

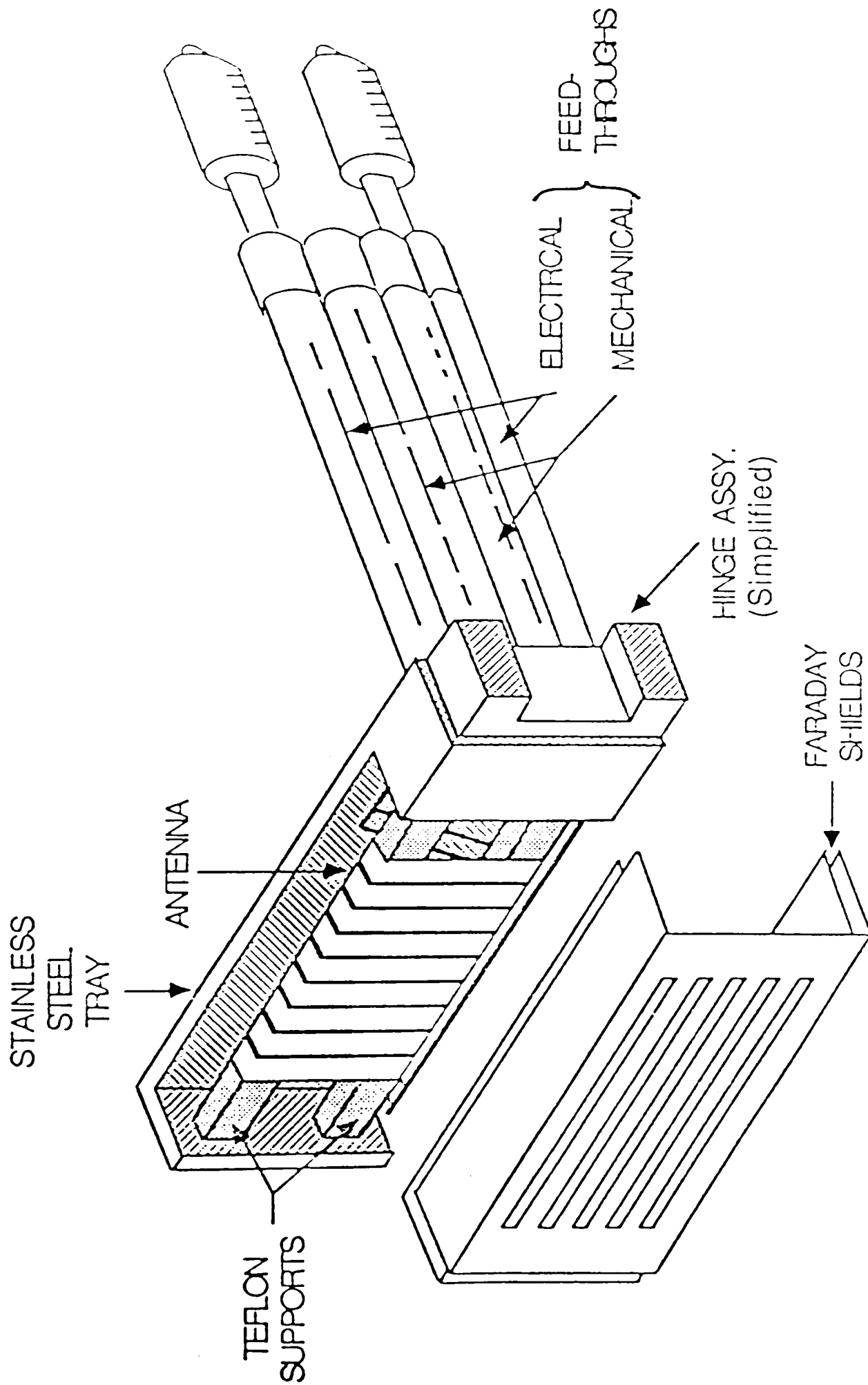


Fig. 8 Original Slow Wave Antenna Assembly.

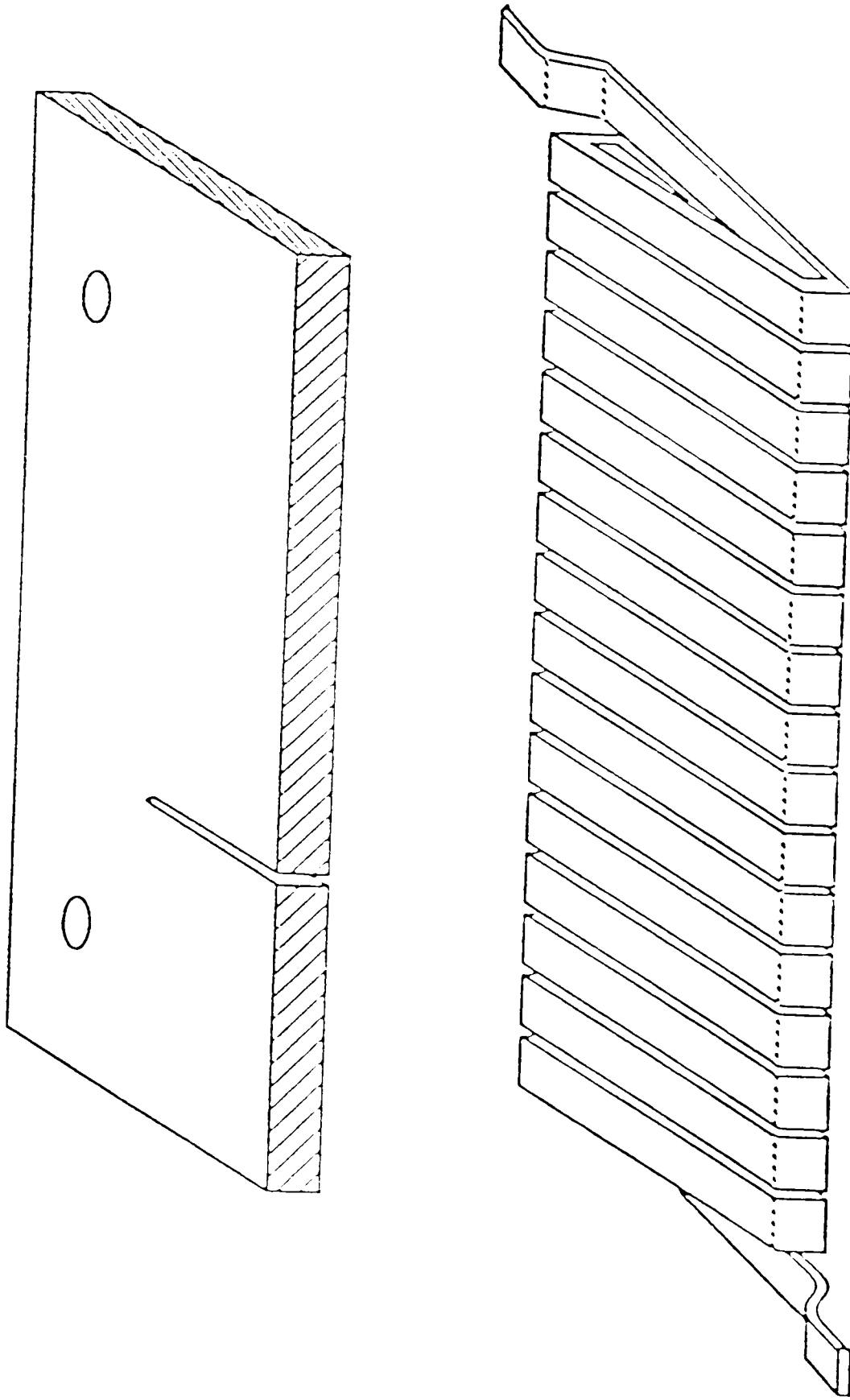


Fig. 9 Stainless Steel Tray and Coiled Slow Wave Structure of Original Antenna.

Another important design consideration for this antenna system is the ease of installation and removal of the antenna. To avoid disassembling the tokamak whenever the antenna is inserted or extracted, the entire antenna assembly is designed to fit through one of the ports on the low field side of the tokamak. Once inside the tokamak, the antenna is rotated 90 degrees so that the axis of the coil is parallel to the plasma column. Two feed-throughs are then plugged into the antenna assembly and tightened down to support the antenna structurally.

Two feed-throughs are used, one for feeding the antenna, the other for removing excess RF power. This design has been used for two basic reasons.

To prevent reflections on the slow wave section of the antenna (the section which radiates to the plasma), the slow wave section must be terminated into 50Ω . Due to physical size constraints, it is impossible to place a 30 kW, 50Ω load resistor in the antenna structure. Therefore, the excess RF excitation on the slow wave structure (that which is not radiated) must be brought out of the machine on a second feed-through so that the slow wave section of the antenna can be properly terminated to prevent reflections.

Secondly, there was no expectation, theoretically, for high power coupling with this antenna. With this antenna design, it is possible to extract any unused power from this antenna and feed this excess power to a similar antenna elsewhere in the machine.

General Results

The original antenna could be matched almost perfectly to the transmission line feeding it. Power reflection was recorded as low as .01%. The antenna stayed nearly perfectly matched regardless of the amount of radiation resistance it encountered. Thirty kW of RF power was easily fed to the antenna with no voltage breakdown. The tokamak was able to maintain a vacuum of 8×10^{-7} Torr after the antenna had been placed within it, an adequate vacuum to operate the machine.

Power coupling was determined by measuring the incident and transmitted current pulses (transmitted current meaning excess current removed from the machine through the second feed-through) with Rogowski coils and by measuring the incident and transmitted voltage pulses with high voltage probes. With plasma in the machine and RF power with a frequency of 6.7 MHz applied to the antenna, power coupling was measured for a variety of incident power levels. The average of the data gives a power coupling of approximately 36%.

Unidirectionality of Wave Propagation in the Tokamak

An experiment was devised to determine whether or not the slow wave antenna actually launches unidirectional Alfvén waves in the Texas Tech Tokamak. Two \dot{B} probes, oriented to detect the B_z component of the fast wave, were

placed near the plasma column, one at a toroidal position of 60° from the antenna, the other at a toroidal position of 90° from the antenna (see Fig.6). The signal from each probe was split and fed to two double balanced mixers. A reference signal, from a Rogowski coil around the incident feed-through of the antenna, was split by a 2-way, 90° splitter. The reference signal was fed to mixer A, which put out the signal $C \cos\phi$. The reference signal shifted by 90° was fed to mixer B, which put out the signal $C \cos(\phi - 90^\circ)$ or $C \sin\phi$. The quantity "C" refers to the amplitude of the probe signal, and " ϕ " refers to the probes' phase difference with respect to the reference signal (see Fig.10).

With $\cos\phi$ and $\sin\phi$ known, ϕ can easily be found. Therefore, as a wave propagates around the machine, the wave's phase difference with respect to the driving RF amplifier can be determined at two distinct points. With this information, the direction of the wave propagation can be discerned.

The results from this experiment are well documented elsewhere^{23,30}. It is sufficient here to say that feeding the slow wave structure RF power at one end resulted in the propagation of a fast Alfvén wave in one direction around the tokamak, while feeding the slow wave structure RF power at the opposite end resulted in the propagation of a fast Alfvén wave, as one would expect, in the other direction around the tokamak.

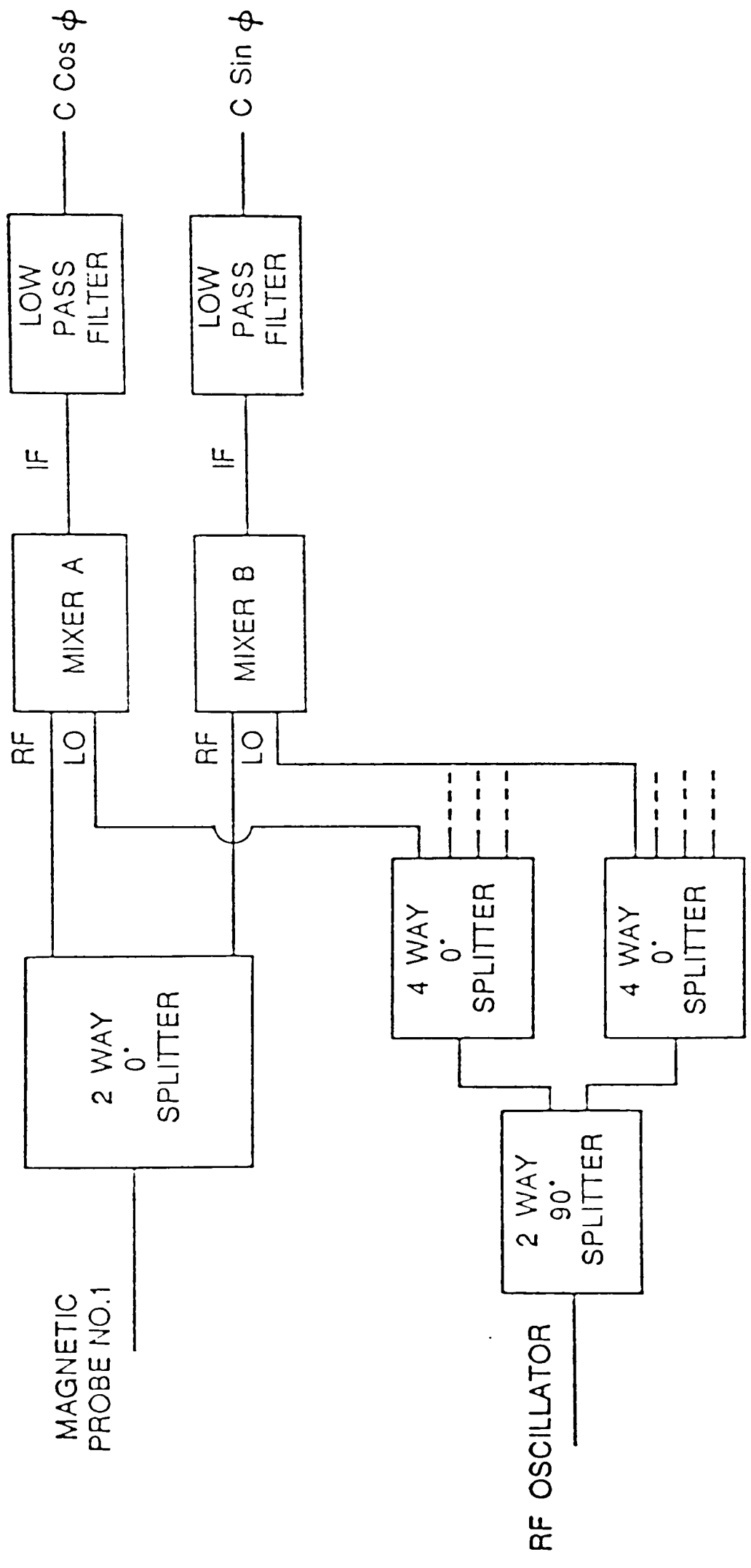


Fig. 10 Phase Comparator Circuitry.

Second Version of Antenna

In an attempt to increase power coupling, a second, longer, but otherwise similar, version of this slow wave antenna was built. Theory predicts²³, and one would expect, that the longer of these slow wave antennas radiates more RF power to the plasma. Figures 11, 12 and 13 depict the second version of the antenna. The antenna's longer length (some 91 centimeters) dictated, for practical reasons, that the antenna lie on the bottom of the machine, in the shadow of the limiter.

This antenna did in fact demonstrate higher power coupling than the original antenna. It coupled approximately 50% of the incident RF power to the plasma. Eventually, up to 40 kW of RF power was supplied to this antenna without electrical breakdown. This longer antenna was used during the experiments described in Chapter 4.

Method of Determination of Current Generation

Characteristics of Current Drive by Asymmetrical Heating of Ions Which Facilitate Determination of Current Drive

Chapter 2 points out that the scheme of current drive by asymmetrical heating of ions, especially in the case of a small tokamak, generates two opposing layers of current. This circumstance, of course, would seem to make

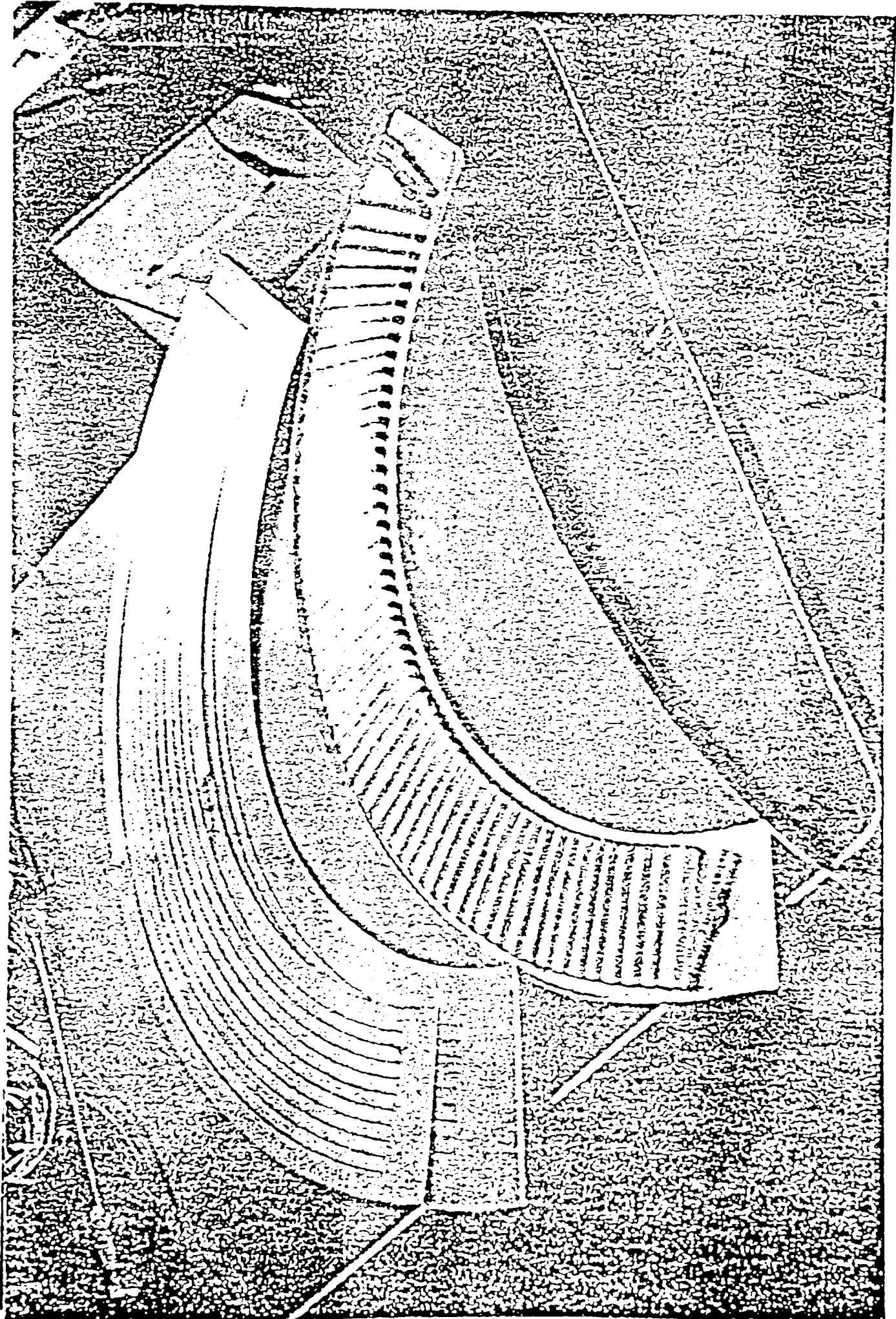


Fig. 11 Photograph of Long Slow Wave Antenna.

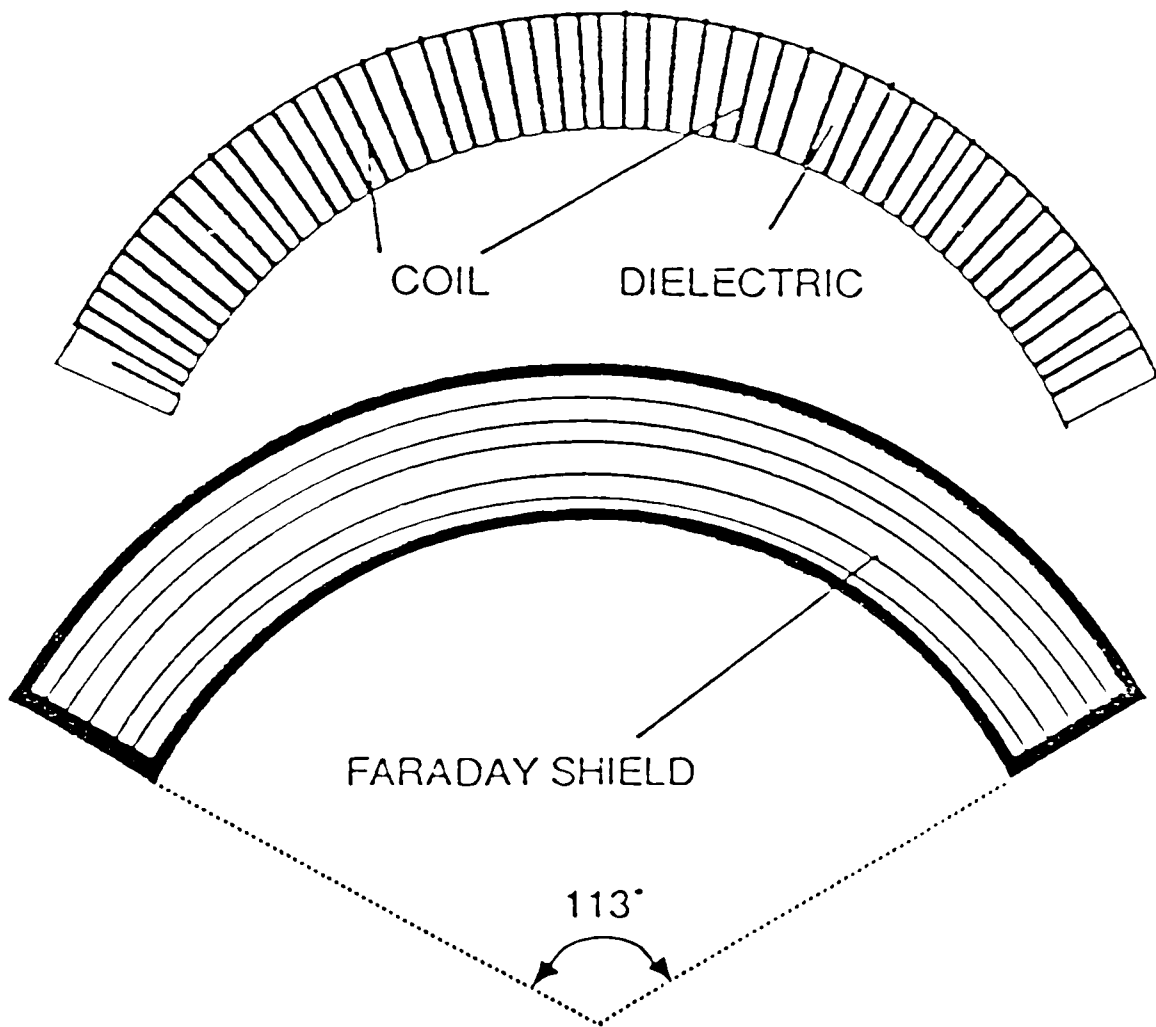
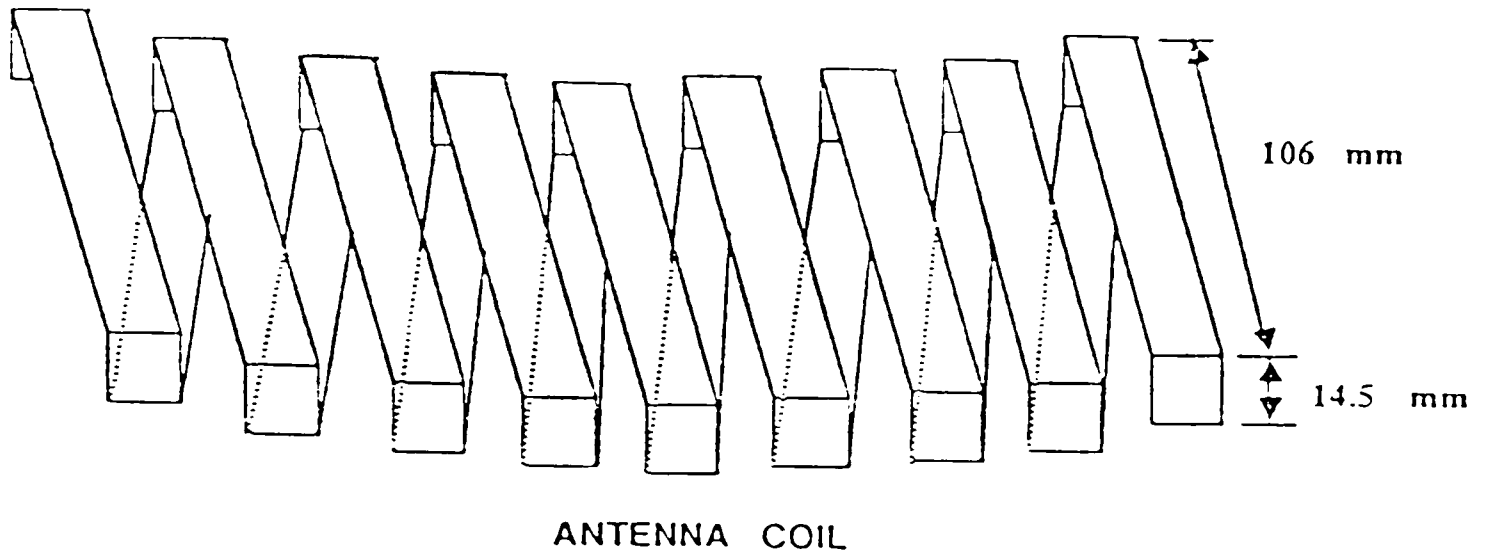


Fig. 12 Diagram of Long Slow Wave Antenna.

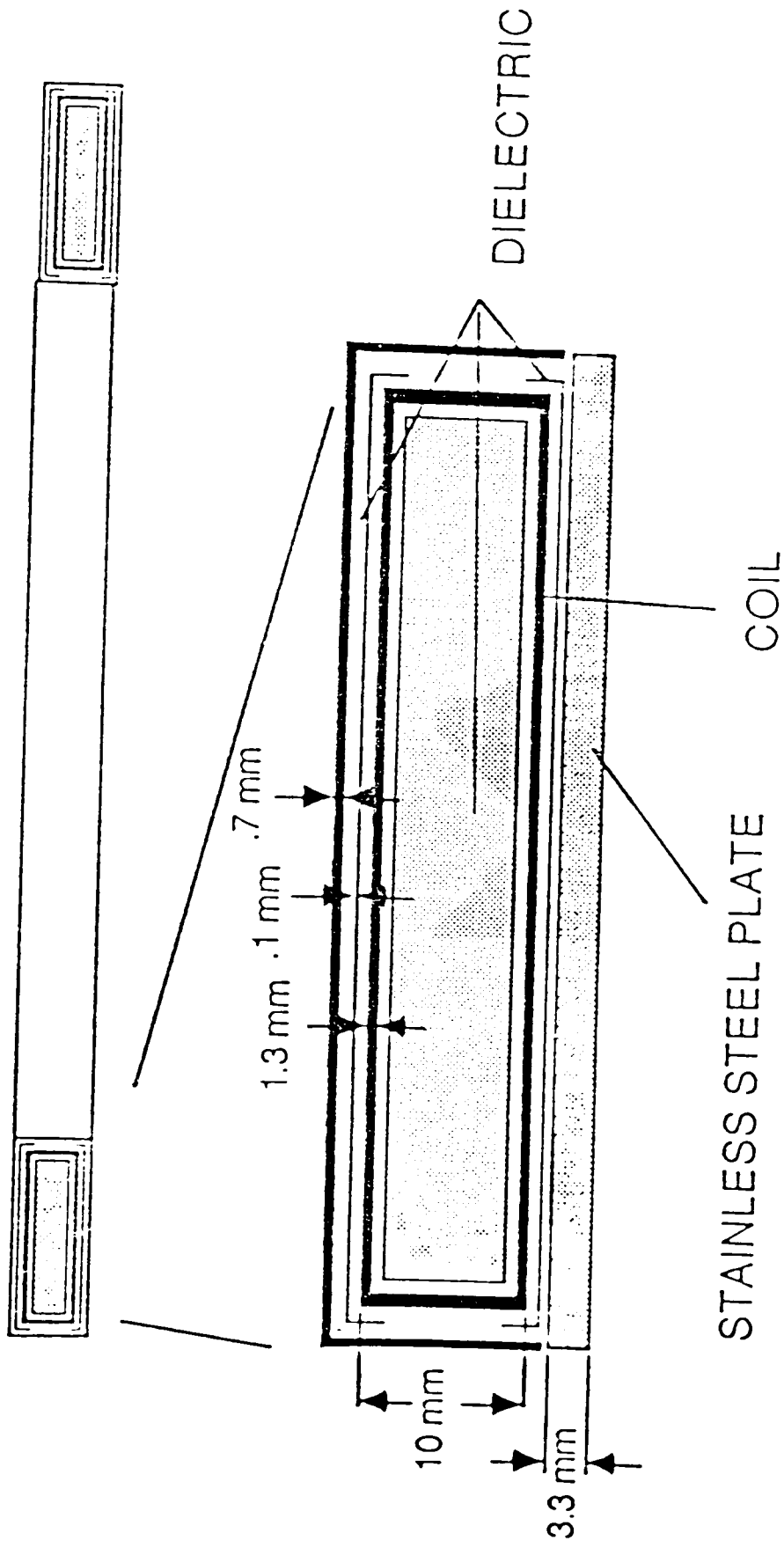


Fig. 13 Cross Section of Long Slow Wave Antenna.

experimental verification of the effect difficult, if not impossible. However, qualities inherent to small tokamaks actually help in the verification of the effect.

The Texas Tech Tokamak has a safety factor, q , of approximately 8 (see Appendix A). This means that a field line makes 8 toroidal transits for every one poloidal transit. The machine is also relatively cold. Calculation of the slow down relaxation rate³¹ of a hydrogen ion (see Appendix B) that has four times the ion thermal velocity on the high field side of the machine shows that, by the time the ion has reached the low field side of the machine, it will have slowed so significantly that it will no longer participate in current generation.

Therefore, during asymmetrical heating on the high field side of the machine, high velocity hydrogen ions heated at the spatial location $\omega = \Omega_L + k_{\parallel} W V_{T\alpha}$ follow the rotationally transformed field lines to the top of the machine and then on to the low field side of the machine. As these particles reach the low field side of the machine, they should slow down, some scattering completely out of the plasma. The high velocity of those particles heated asymmetrically makes current generation possible. Hence there should be a region of greater current generation towards the top of the machine, where particles have not slowed significantly (see Fig. 14).

Similarly, during asymmetrical heating on the high field side of the machine, high velocity hydrogen ions

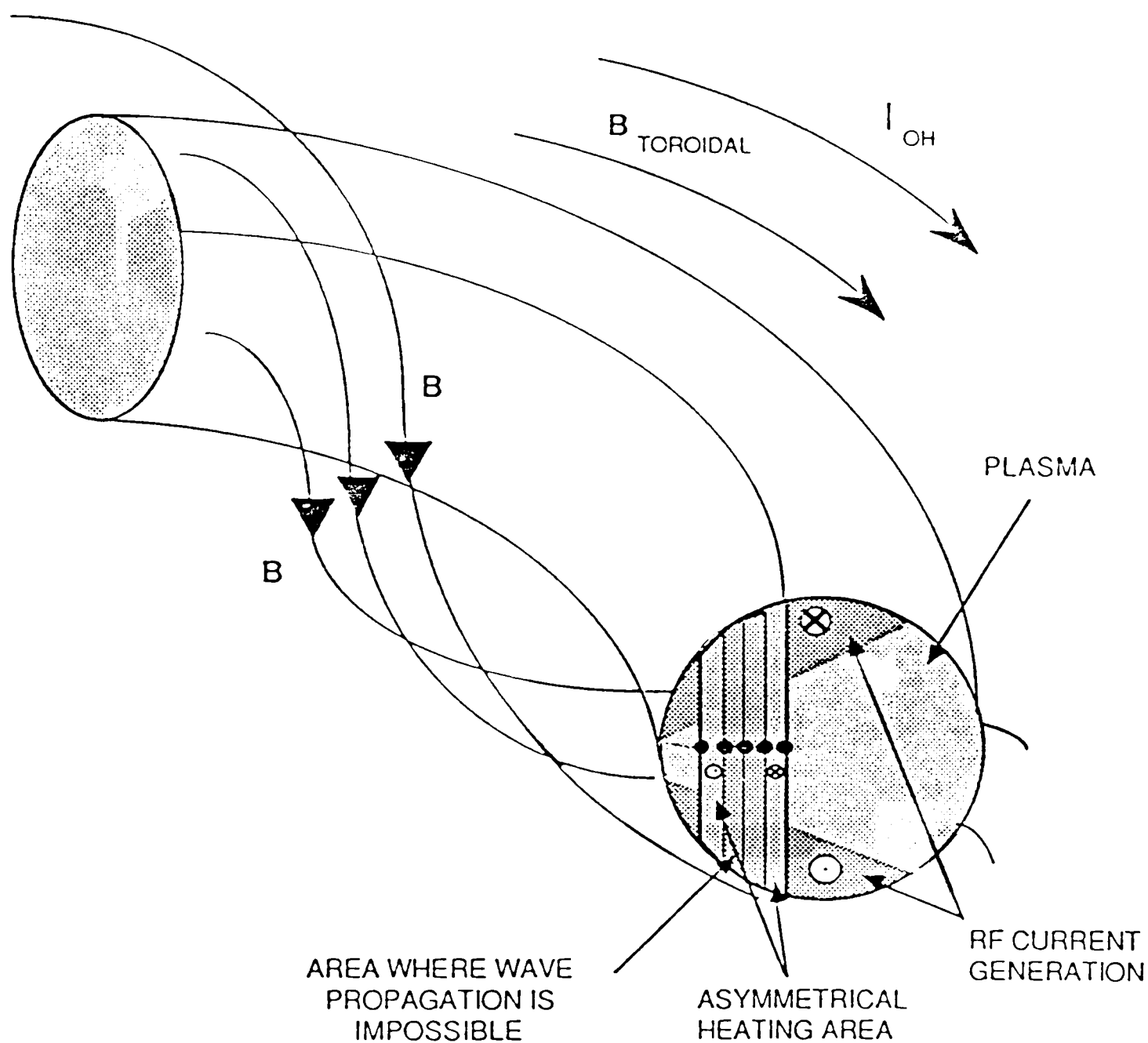


Fig. 14 Section of Tokamak Plasma Showing Area of Asymmetrical Heating, Area of Wave Cut-off, Areas of RF Current Generation, Direction of I_{OH} (Ohmic Heating Current), and Rotational Transform of the Machine (Which is Exaggerated for Purposes of Demonstration).

heated at the spatial location $\omega = \Omega_L - k_{\parallel} W V_{T\alpha}$ follow the rotationally transformed field lines to the bottom of the machine and then on to the low field side of the machine. As these particles reach the low field side of the machine, they should also slow down, some scattering completely out of the plasma column. Again the high velocity of those particles heated asymmetrically makes current generation possible. Hence there should be a region of greater current generation towards the bottom of the machine, where particles have not slowed significantly. The current generated near the bottom of the machine is in the direction opposite to that current generated near the top of the machine (see Fig. 14).

Current will flow out of these areas of current generation towards the low field side of the machine. However, since the two areas of current generation drive currents in opposite directions, the two currents cancel. The current within the two areas of current generation should however, perturb the current density profile of the column.

Apparatus and Procedure Used to Determine Current Drive

To observe current drive by asymmetrical heating of ions in the Texas Tech Tokamak, two current probes (\dot{B} probes) are placed at the top and bottom of the plasma column, just outside of the plasma (see Fig. 15). The \dot{B}

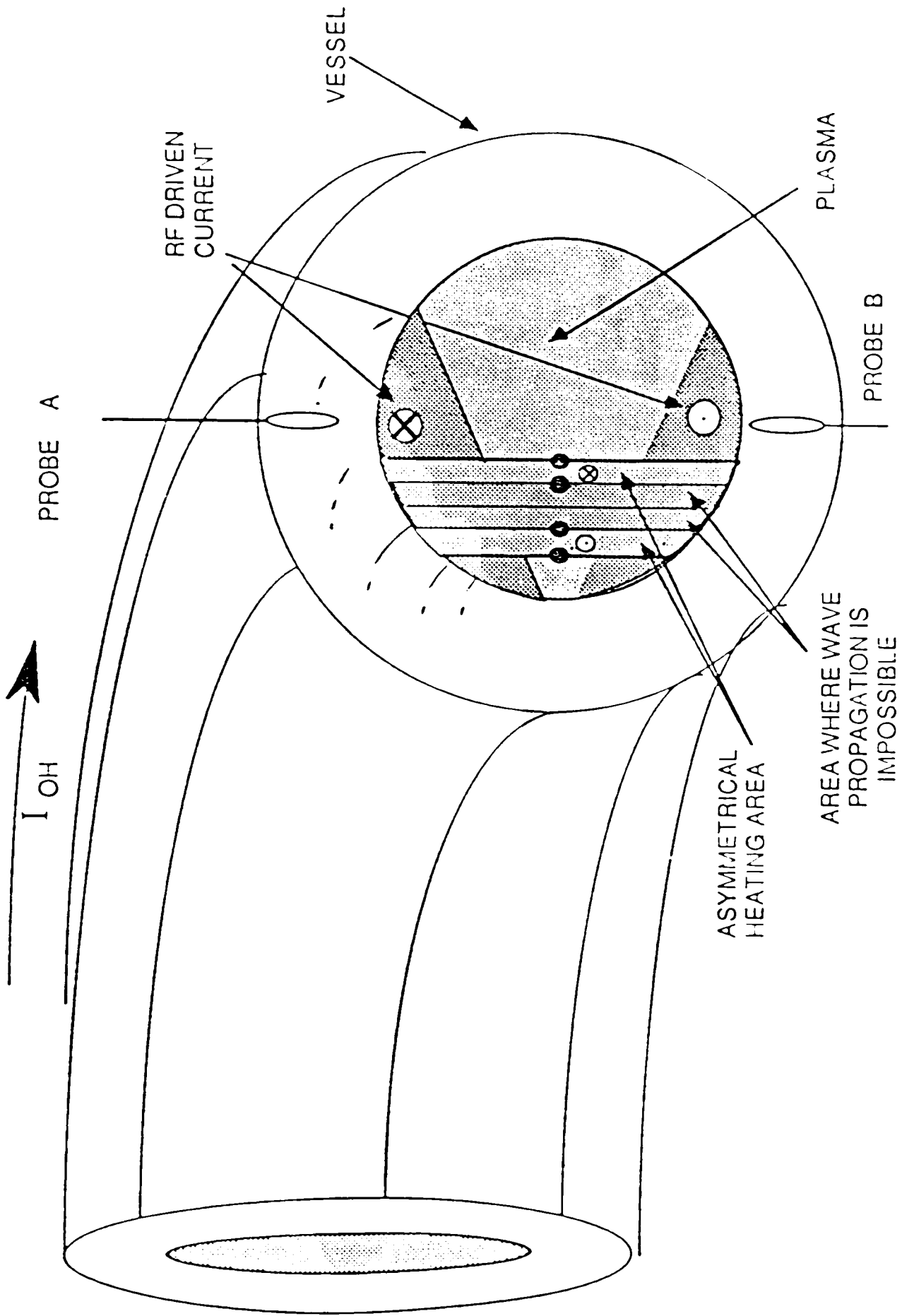


Fig. 15 Section of Tokamak Showing Location of Current Probes in Relation to Plasma Column.

probes are oriented so that they detected the current in the plasma column and not the magnetic field of the Alfvén wave. In fact, the current probes are low-pass filtered to ensure the elimination of any effect from the magnetic field of the fast Alfvén wave. Figure 16 shows the top view of the vacuum vessel with the relative toroidal positions of the current probes and the slow wave antenna. The current probes are purposely placed on the side of the torus opposite the antenna to prevent any near field antenna effects from corrupting the data.

The signals from the current probes are sent to a differential amplifier, where the difference between the signals is amplified and recorded. If any "up-down" variation in the current density of the plasma column were to occur, this diagnostic would detect it.

Recall from the previous section that the ohmic heating current in the tokamak for this experiment is in the direction of the postulated RF driven current generated at the bottom of the machine. Label the probe at the top of the plasma column 'A' and the probe at the bottom of the plasma column 'B'. The RF driven current near probe 'A' would be in a direction opposite to that of the ohmic heating current; hence, the signal 'A' would decrease. At the same time, RF driven current near probe 'B' would be in the same direction as the ohmic heating current; hence, the signal 'B' would increase, with the overall effect

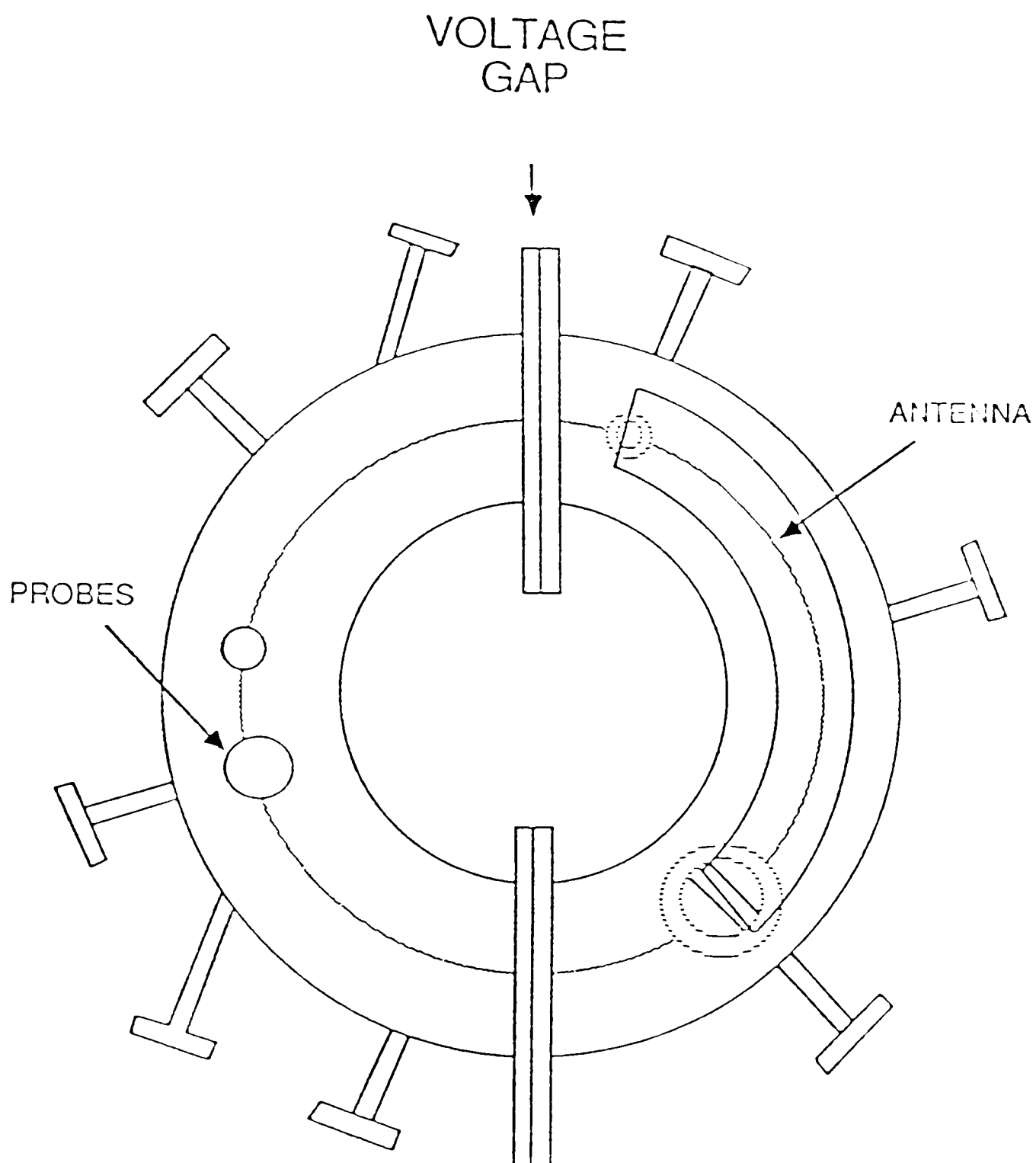


Fig. 16 Top View of Texas Tech Tokamak Vacuum Chamber With Relative Position of Long Antenna and \dot{B} Probes.

that the signal 'A' - 'B' would decrease. If the signal from the differential amplifier, 'A' - 'B', goes negative during RF heating, therefore, then the postulated effect must be occurring (see Fig. 15).

CHAPTER IV

RESULTS

General Results

Figure 17 shows typical experimental data from two tokamak shots. The data are the differential amplifier response, 'A' - 'B', described in the previous chapter.

When RF power with a frequency of 9.7 MHz was applied to the antenna and a fast Alfvén wave launched in the tokamak, the signal 'A' - 'B' appeared no different than when no RF was applied to the antenna and no wave launched. This observation is consistent with the fact that the spatial location of the fundamental cyclotron resonance for hydrogen is well "outside the machine" at 9.7 MHz. Therefore, asymmetrical heating is impossible; consequently, no current generation; no current density asymmetry of the plasma column; and hence no deflection of the probe signal 'A' - 'B' occurs.

However, application of RF power at 7.7 MHz to the antenna launched a fast Alfvén wave that could heat ions asymmetrically on the high field side of the machine. At 7.7 MHz the spatial location of the fundamental cyclotron

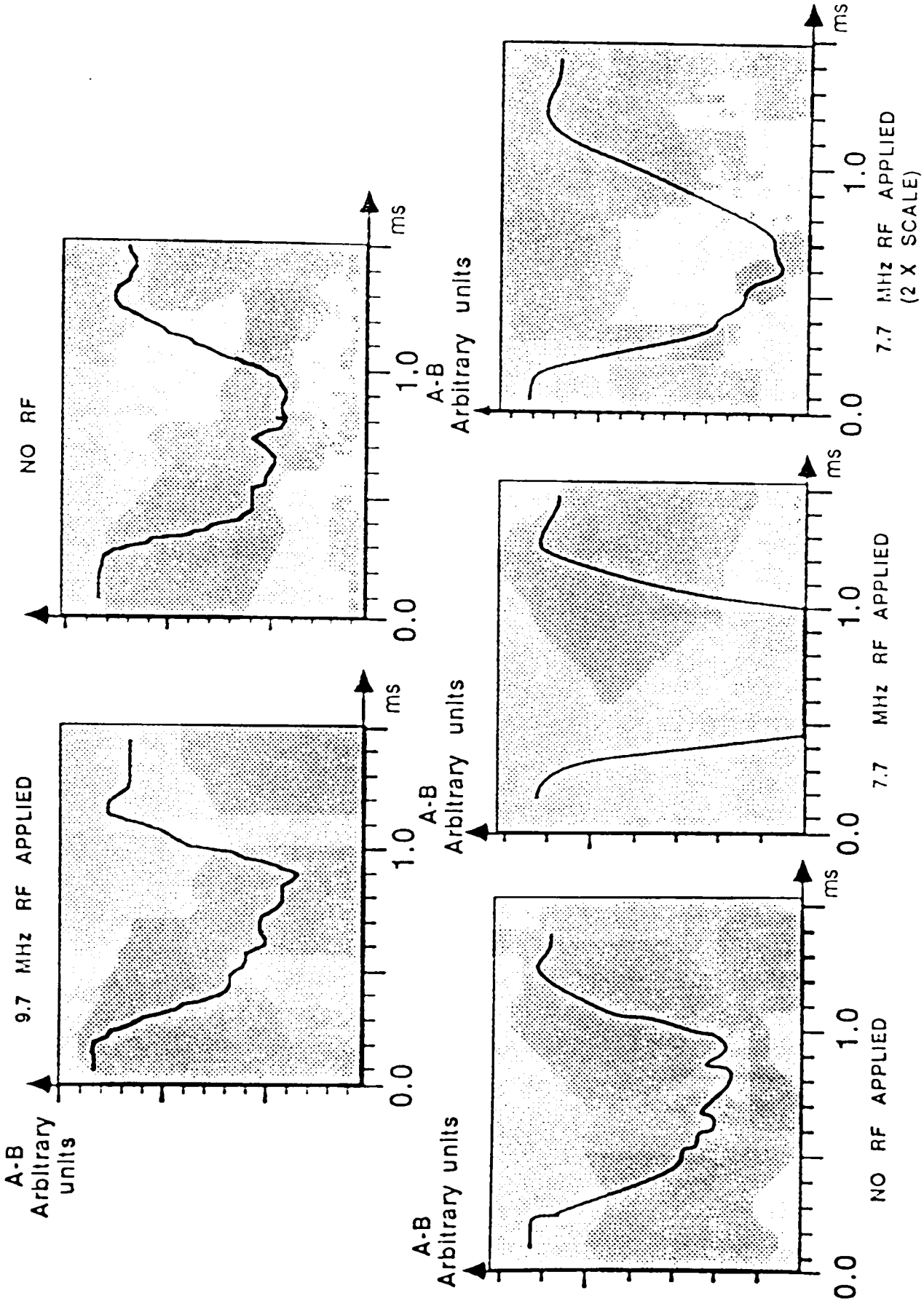


Fig. 17 Typical Experimental Data, Probe Signal 'A'-'B', Which Depicts Asymmetry of Current Density in Plasma Column. RF at 9.7 MHz Places Heating Layer 'Outside' Machine, RF at 7.7 MHz Places Heating Layer 'Inside' Machine.

resonance for hydrogen is "in the machine" on the high field side. Figure 17 shows that the probe signal 'A' - 'B' is clearly more negative with the application of RF at 7.7 MHz than when no RF is applied. The probe signal 'A' - 'B' therefore indicates an asymmetry of the current density in the plasma column, caused by the postulated current drive effect. Even though there was a heating layer within the machine, there appeared to be no substantial alteration in the mode structure of the fast Alfvén wave.

Figure 18 shows the signal response, 'A' - 'B', versus frequency. At about 8.5 MHz the signal 'A' - 'B' starts to go negative. This observation corresponds to the entrance of the asymmetrical heating layer into the machine from the high field side. As the applied frequency decreases, the asymmetrical heating layer moves deeper into the machine. The area of possible current generation becomes greater towards the poloidal axis of the machine and the possibility that particles which participate in current generation scatter out of the machine becomes less as the heating layer approaches the poloidal axis of the machine. Therefore, the response 'A' - 'B' becomes more negative as the frequency decreases and the heating layer moves toward the poloidal axis.

From an argument similar to one already given, the probe response 'A' - 'B' should go positive if the asymmetrical heating layer lies on the low field side of the

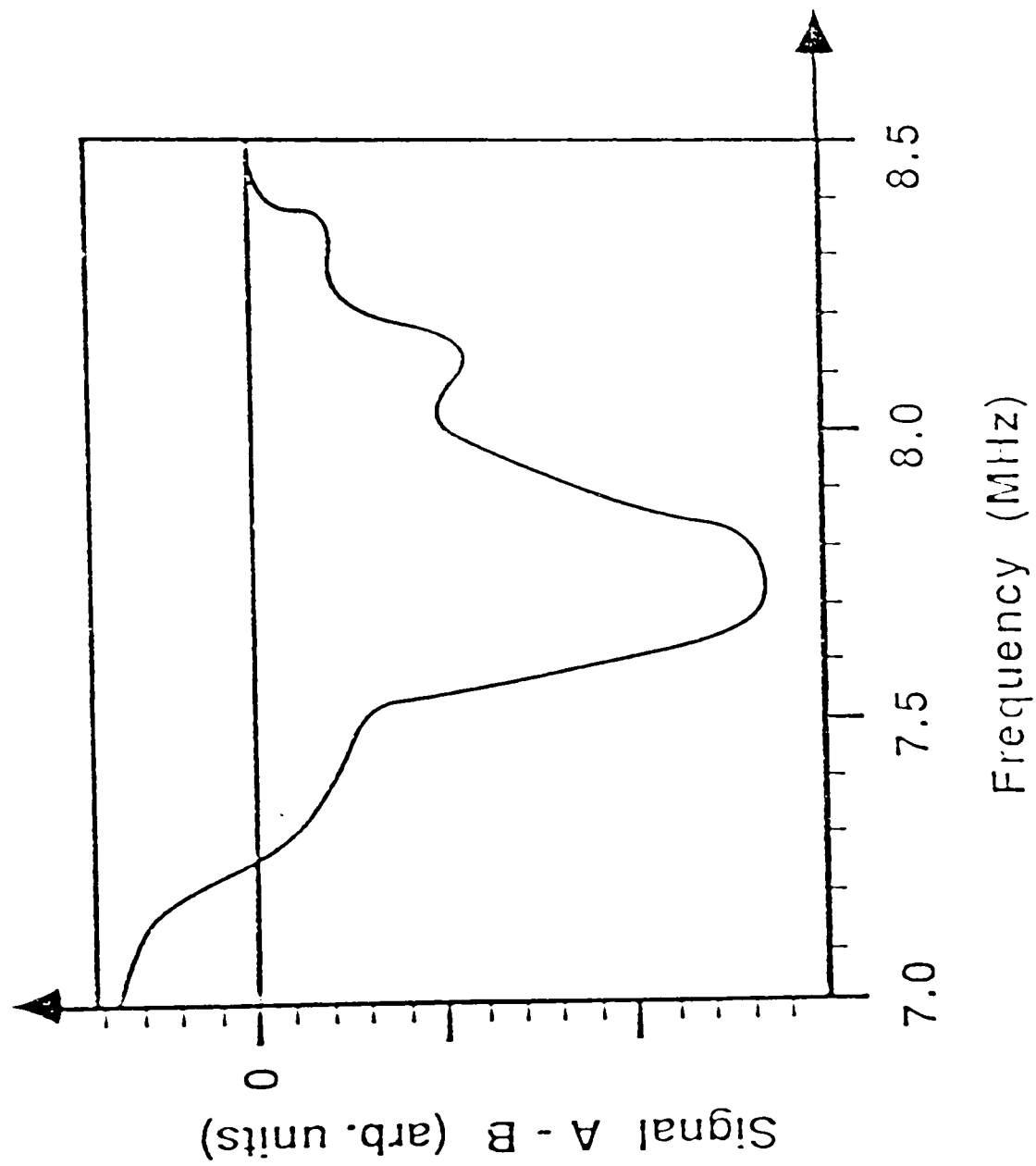


Fig. 18 Probe Signal 'A'-'B'. Plotted as a Function of Frequency.

machine. From Fig. 18 one can see that the probe response 'A' - 'B' does indeed go through zero and become positive as the heating layer reaches the poloidal axis (corresponding to $f \approx 7.2$ MHz) and moves on to the low field side of the machine.

Figure 19 shows the result of a tokamak shot in which the frequency of the RF power supplied to the antenna was modulated between 7.5 and 8.1 MHz. This modulation was possible since a wide band, slow wave, transmission line type antenna (described in Chapter 3) was used. This modulation in frequency moved the heating layer repeatedly from the outside edge of the plasma column towards the poloidal axis of the machine. Note that the response 'A' - 'B' followed the modulation in frequency exactly.

Analysis of Results

One of the obvious questions at this point is "what is the experimental efficiency of this current drive scheme?" Unfortunately, neither the experimental setup used to demonstrate the effect nor practical modifications of the setup lend themselves to easy or accurate estimates of the current drive efficiency.

The magnitude of the signal 'A' - 'B', corrected for noise, was at its maximum, approximately ten times smaller than the magnitude of either the signal 'A' or 'B'. Since the probes 'A' and 'B' were looking at the total

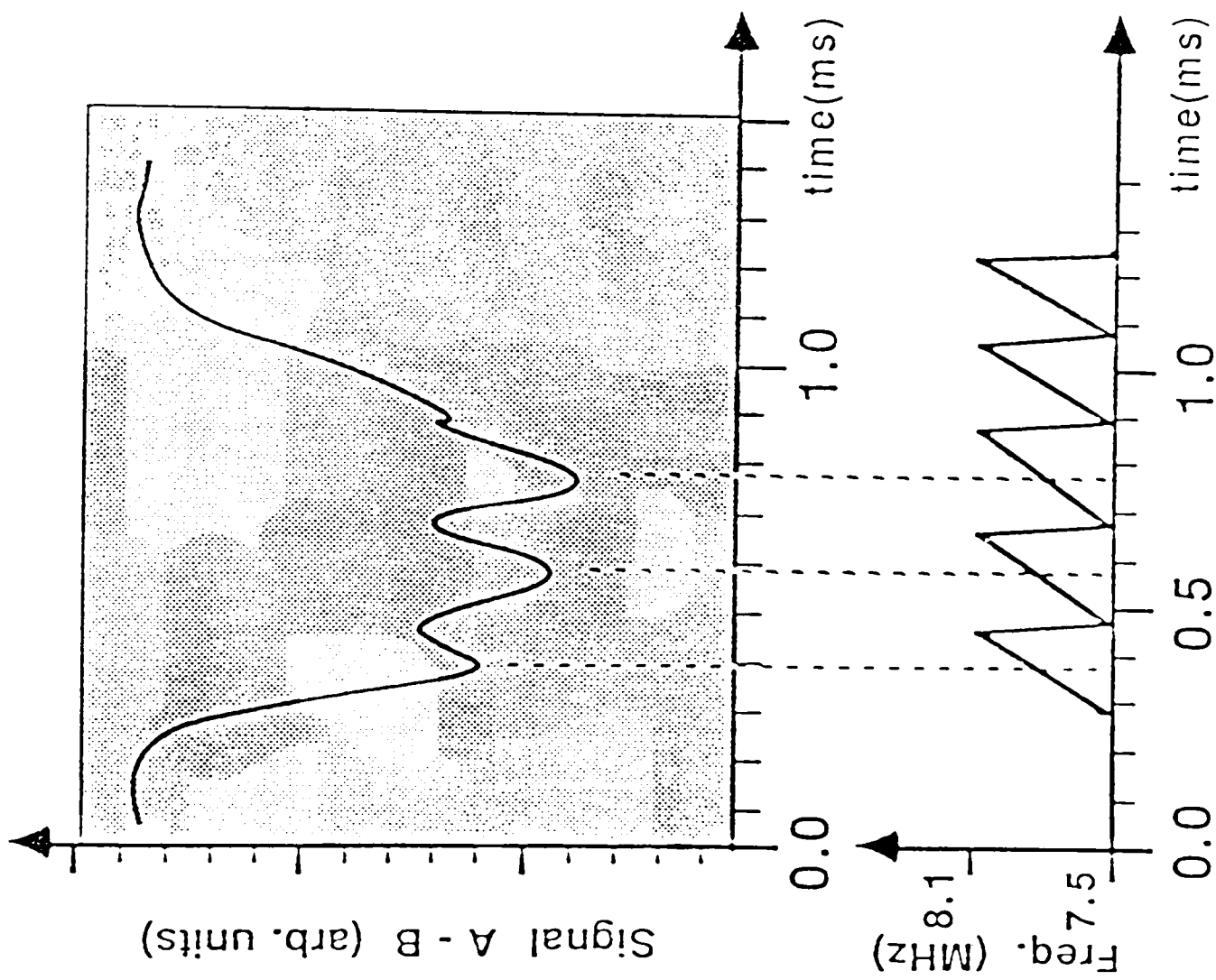


Fig. 19 Probe Signal 'A'-'B' During Tokamak Discharge in Which RF Was Modulated Between 7.5 and 8.1 MHz.

plasma current, which was 10 kA, one might be tempted to say that the total RF driven current (represented by the signal 'A' - 'B') was therefore approximately 1 kA. This conclusion, unfortunately, would be incorrect.

It is well known that the current density in a tokamak plasma is much greater at the poloidal axis of the tokamak than at the edges of the plasma column. In fact, a plot of current density versus radial position would be quite peaked at the center of the plasma column. The 10 kA of current that the probes 'A' and 'B' detected was (taking a crude guess) some 13 cm away from the probes.

The RF driven current on the other hand, should have been, as discussed in Chapter 3, rather close to the edge of the plasma column and hence rather close to the probes. Herein lies the problem: it is not really known exactly where the RF driven current flows (meaning, how close to the probes it lies). If one makes a crude guess that the RF driven current is some 1.3 cm away from the probes, and if one recalls the previous guess that the bulk of the ohmically driven current is some 13 cm away from the probes, then the probes' sensitivity to the RF driven current is ten times greater than their sensitivity to the ohmically driven current (the magnetic fields of the currents should drop as $1/r$). Thus, although the magnitude of the signal corresponding to RF driven current ('A' - 'B') may have been one-tenth of the magnitude of the signal corresponding

to the ohmically driven current ('A' or 'B'), the probes' ten times greater sensitivity to the RF driven current than to the ohmically driven current could mean that the RF current drive accounts for maybe only one-hundredth of the ohmically driven current.

This means that when 40 kW of RF power was applied to the slow wave antenna and approximately 20 kW of RF power was injected into the plasma, only about 100 A of RF driven current, in the maximum case, was obtained. This works out to an efficiency of approximately 5 mA of toroidal current generated for each watt of RF power used.

In Chapter 2, a theoretical efficiency for this current drive scheme was calculated using a one-species, hydrogen plasma. Utilizing Fisch's corrected theory, a value of 30 mA of toroidal current for each watt of RF power used was obtained. Therefore, the extremely crude determination of the experimental efficiency corresponds relatively well to the simple theoretical calculation of efficiency.

Wong³², in a more sophisticated, numerical calculation based on the Fokker-Planck equation, calculated the current drive efficiency for the one-species (hydrogen) current drive scheme, in the Texas Tech Tokamak to be approximately 18 mA of toroidal current for each watt of RF power used. This result gives added confidence in the relatively crude calculations presented here.

One minor unexpected result was that the magnitude of the differential amplifier signal $|'A' - 'B'|$ (corresponding to RF current drive) was smaller when asymmetrical heating occurred on the low field side of the machine (see Fig. 18). One possible explanation for this finding (known from personal experimental experience and also from Coleman¹¹) is that the fast Alfvén wave simply does not propagate very well in the Texas Tech Tokamak at frequencies much below 7 MHz. This circumstance could of course make current drive difficult on the low field side of the machine, since the local cyclotron frequency for hydrogen is below 7 MHz on this side of the tokamak. Another possible explanation for this finding is that this current generation scheme is simply less efficient on the low field side of the tokamak. Hamnen³³ has predicted this very effect to occur for Fisch's original current drive scheme if it is attempted on the JET tokamak.

Finally, it is clear that the signal $'A' - 'B'$ has detected current asymmetry and not simply gross column movement. It is true that the application of RF power to a plasma column can cause the column to move. However, Fig. 19 shows that slight variation in the frequency of the applied RF power causes a large variation in the signal $'A' - 'B'$, a phenomenon which is unexplainable in the context of plasma column movement.

CHAPTER V

CONCLUSIONS

It has been shown that current drive by asymmetrical heating of ions in a tokamak plasma is in fact an observable physical phenomenon. Unfortunately, this current drive scheme does not seem to be a likely candidate for the primary means of current generation in tokamaks for a variety of reasons. Aspects of this current drive scheme may warrant further investigation however.

A General Assessment of Current Drive by Asymmetrical Heating of Ions

Parameters common to small tokamaks ($T_e > T_i$, $Z_{eff} > 1$) tend to severely degrade the efficiency of current drive by asymmetrical heating of ions, which was not considered in the original proposed scheme by Fisch. Added to this problem of low efficiency is the fact that Fisch's scheme may be severely hampered, if not made impossible, by the absorption of RF power by the bulk plasma at the minority species resonance. This circumstance, as a practical matter, is virtually unavoidable in a small machine. Even for the observed, one-species current drive scheme, the fact that the electron temperature is greater

than the ion temperature causes the efficiency of this current drive scheme also to be very low.

It would appear that large tokamaks would not be hampered by these temperature and effective charge effects, and that the current drive efficiency in these type of machines could be rather large. Fisch predicted⁸ (in a calculation which he termed 'crude') that in a large "PLT type machine," his current drive scheme would have an efficiency of approximately .5 A of toroidal current generated for each watt of RF power used. Wong predicted³² using a numerical Fokker-Planck calculation, that in a large "generic type" tokamak, the one-species (hydrogen) current drive scheme demonstrated in the Texas Tech Tokamak would have an efficiency on the order of 1 amp of toroidal current generated for each watt of RF power used.

The problem with these efficiency calculations is that values for the tokamak parameters are chosen so as to optimize current drive efficiency with little thought as to whether these values are necessarily obtainable simultaneously or are sustainable throughout the tokamak discharge. Variation in some of these parameters can cause drastic reduction in the current drive efficiency. It is extremely difficult to control the values of some of these parameters, especially when it is also extremely difficult to determine their values.

One example of a parameter which is difficult to control is the effective charge of a tokamak plasma. We have seen in Chapter 2 what a drastic effect this parameter can have on current drive efficiency. In large machines the effective charge of the plasma, Z_{eff} , is known to be greater than 1, though how much greater is difficult to determine, even with sophisticated diagnostic equipment. It is known on JET (the Joint European Tokamak)³⁴ for example, that Z_{eff} increases slightly during RF heating, and increases gradually from shot to shot. Various techniques, such as carbonization of the inner walls of the tokamak, decrease Z_{eff} , but by how much is unpredictable, and the effect is temporary in any case.

As difficult as the control of various plasma parameters may be, the real difficulty with current drive by asymmetrical heating of ions when considered as a candidate for primary current drive in large tokamaks, is the spatial localization of the current drive associated with this scheme. As mentioned several times before, current generation occurs in this scheme at the spatial locations inside the tokamak which satisfy $\omega = \Omega_L \pm k_{\parallel} W V_{T\alpha}$ where ω is the frequency of the applied RF power, k_{\parallel} is the parallel wave number, and $W V_{T\alpha}$ is some multiple of the ion thermal velocity. If the primary current of the tokamak is to be generated by this scheme, only one of the relations, $\omega = \Omega_L + k_{\parallel} W V_{T\alpha}$ or $\omega = \Omega_L - k_{\parallel} W V_{T\alpha}$ can be satisfied within

the tokamak; otherwise, two opposing layers of current are generated within the machine, resulting in no overall current generation. Furthermore, if Fisch's original scheme is used, the spatial location where $\omega = \Omega_L$ is satisfied must also be kept out of the plasma column to prevent simple bulk heating at the minority species resonance from "eating up" the RF power.

In the Texas Tech Tokamak the term $k_{\parallel} W V_{T\alpha}$ is very small compared to Ω_L , thus placing the two opposing asymmetrical heating layers spatially close together. It is true that, in large machines, $V_{T\alpha}$ will be some 20 times larger than in the Texas Tech Tokamak. However, in large machines, the term Ω_L (a function of toroidal magnetic field) is also larger than in the Texas Tech Tokamak, perhaps some 10 times bigger. So even in large machines (if k_{\parallel} is of about the same order as in the Texas Tech Tokamak) $\Omega_L \gg k_{\parallel} W V_{T\alpha}$.

It appears likely, that if only one of the relations $\omega = \Omega_L + k_{\parallel} W V_{T\alpha}$ or $\omega = \Omega_L - k_{\parallel} W V_{T\alpha}$ is satisfied in a large machine, it will be satisfied near the edge of the plasma column, with the other relation satisfied just outside the column. If current drive by asymmetrical heating is to be the only means of current generation employed within the tokamak, current density within the plasma column would be concentrated near the edge of the plasma column. This current density profile would be very unusual for a tokamak, and could lead to difficulties with plasma stability.

Peculiarities of Current Drive by
Asymmetrical Heating of Ions Which
Warrant Further Investigation

Even though current drive by asymmetrical heating of ions may not prove to be a means of generating the bulk of a tokamak's current, its spatially localized nature could permit the current density profile of a tokamak's plasma column to be tailored to suit the experimenter's needs. The experimenter could even vary the current density profile as a function of time by simply modulating the frequency of the RF excitation (as discussed in Chapter 4).

As mentioned before, current density profiles of tokamak plasma columns are peaked at the poloidal axis of the machine. An interesting experiment would be to generate a current layer right at the edge of the plasma column. Once the current density profile had been perturbed in this way, it would be interesting to see if the perturbed current density profile would relax to its original shape. If this relaxation did indeed occur, it would indicate that the original current profile was a preferred state for the plasma to be in, associated with a so called "Taylor relaxed state"³⁵. This question has never been investigated experimentally for a tokamak and is currently an area of intense interest in plasma physics.

One other interesting experiment is the use of spatially localized current generation to maintain MHD stability in large tokamaks. As large tokamaks are pushed towards ignition, current density in the machines must be

increased to heat the plasma contained within them. But, because current density profiles are so peaked at the poloidal axis of tokamaks, the current density at the poloidal axis becomes very large, causing the safety factor q (which is inversely proportional to current) to be driven to less than 1 at the poloidal axis. This condition permits MHD instability and the rapid cooling of the tokamak plasma to occur³⁶.

A possible experimental approach is illustrated in Fig.20. Two opposing layers of current are generated within the machine. One layer, positioned at the poloidal axis of the machine, would oppose inductively driven current in the column, therefore reducing the current density at the poloidal axis, and increasing the value of the safety factor q , and thereby maintaining MHD stability throughout the plasma column. At the same time, another current generating layer, driving current in the same direction as the inductively driven current, would be introduced nearer the edge of the plasma column. Here, current density is normally low, and therefore the increase in current density at this location has no effect on MHD stability. In this way, the current inductively driven in the tokamak could be increased to heat the plasma without driving the plasma into MHD instability, since spatially localized current (generated by asymmetrical heating of ions) "flattens out" the current density profile of the plasma column, as shown in Fig.20.

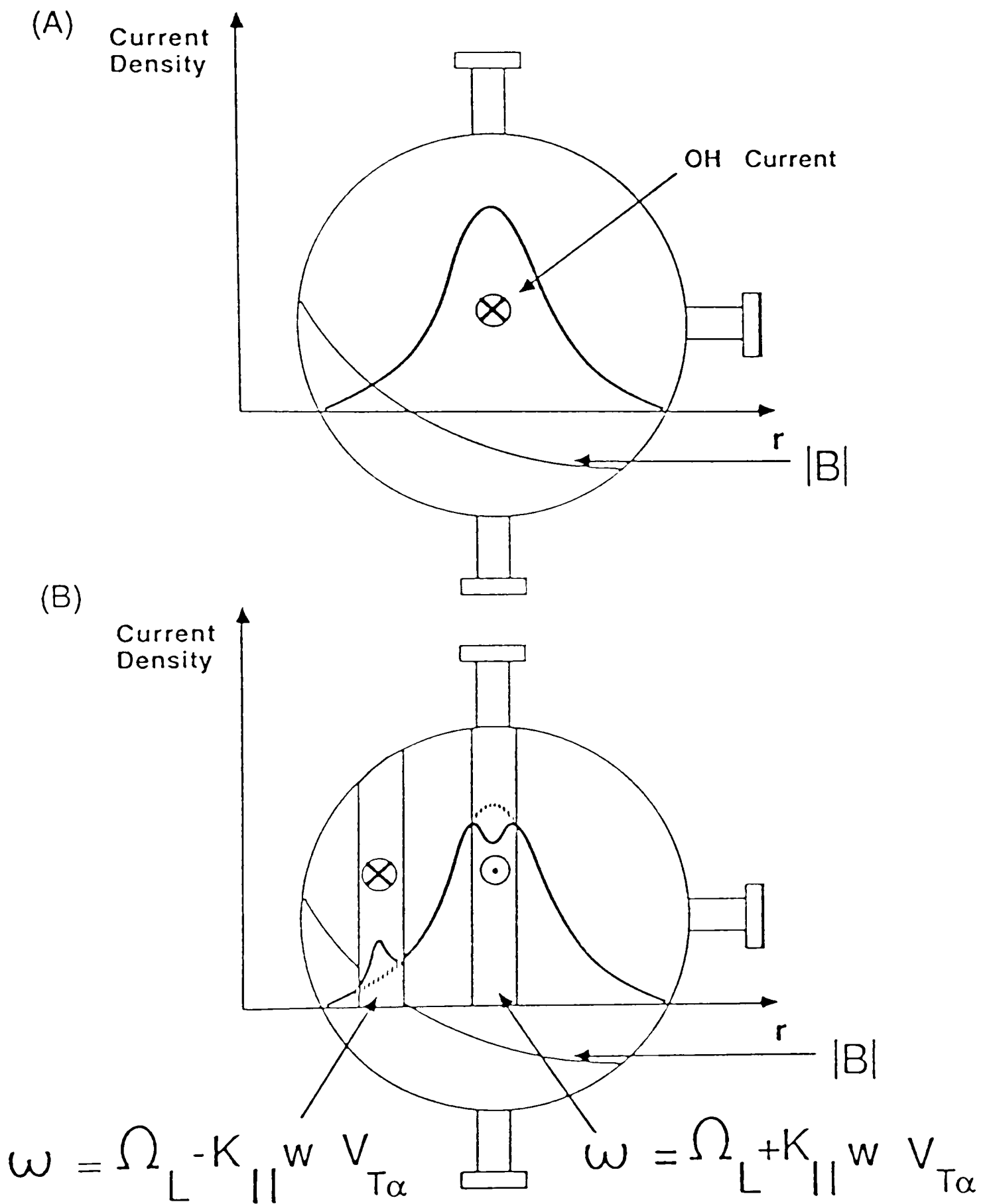


Fig. 20 Cross Section of a Tokamak Showing Current Drive by Asymmetrical Heating of Ions Flattening the Current Density Profile of a Tokamak Plasma Column.

LIST OF REFERENCES

1. D. J. H. Wort, Plasma Phys., 13, 258 (1971).
2. T. Ohkawa, Nucl. Fusion, 10, 185 (1970).
3. N. J. Fisch, Phys. Rev. Lett., 41, 873 (1978).
4. D. Jassby, Nucl. Fus., 17, 309 (1977).
5. T. Yamamoto, et. al., Phys. Rev. Lett., 45, 716 (1980).
6. C. F. F. Karney and N. J. Fisch, Phys. Fluids, 22, 1817 (1979).
7. J. Goree, et al., Phys. Rev. Lett., 55 , 1669 (1985).
8. N. J. Fisch, Nucl. Fusion, 21, 15 (1981).
9. B. A. Trubnikov, Review of Plasma Physics, Ed. by M. A. Leontovich, (Consultants Bureau, New York, Vol. 1, 1965), p. 105.
10. J. Hosea, et al., in the Proc. Fourth International Symposium on Heating in Toroidal Plasmas, (Rome, Italy, 1984).
11. P. D. Coleman, "Propagation and Damping of the Fast Alfvén Wave in the Texas Tech Tokamak," Ph.D. Dissertation, Dept. of Elect. Engr., Texas Tech University (1983).
12. D. A. Ehst, et al., A Demonstration Tokamak Power Plant Study (Argonne National Laboratory, 1982) p. 2-54.
13. P. C. Efthimion, et al., "Initial Confinement Studies of Ohmically Heated Plasmas in the Tokamak Fusion Test Reactor," Tech Report, PPPL-2078, Princeton Plasma Physics Laboratory, June 1984, Princeton, New Jersey.
14. B. E. Keen and P. Kupschus, "JET Joint Undertaking Progress Report," Tech Report, EUR 10223 EN (Eur-JET-PR2), JET Joint Undertaking, September 1985, Abingdon, Oxon., England.

15. M. Yoshikawa, Bull. Am. Phys. Soc., 30, 1362 (1985).
16. F. W. Perkins, Nuclear Fusion, 17, 1197 (1977).
17. J. Gahl, et al., "Experimental Observation of Current Generation by Asymmetrical Heating of Ions in a Tokamak Plasma", submitted for publication in Journal of Applied Physics.
18. T. H. Stix, Nucl. Fusion, 15, 737 (1975).
19. T. H. Stix, The Theory of Plasma Waves (McGraw-Hill, New York, 1962).
20. J. E. Cato, "Plasma Heating and Wave Damping Near Harmonics of the Ion Cyclotron Frequency," M.S. Thesis, Dept. of Elec. Engr., Texas Tech University (1969).
21. B. D. Fried and S. D. Conte, The Plasma Dispersion Function (Academic Press, New York and London, 1961).
22. P. D. Coleman, "Probe Measurements of the Magnetic Structure of Fast Wave Toroidal Eigenmodes," M.S. Thesis, Dept. of Elec. Engr., Texas Tech University (1980).
23. J. Gahl, "Antenna for Unidirectional Propagation of Fast Alfvén Waves in a Small Tokamak," M.S. Thesis, Dept. of Elec. Engr., Texas Tech University (1982).
24. H. C. Kirbie, "Design and Construction of the Texas Tech Tokamak," M.S. Thesis, Dept. of Elec. Engr., Texas Tech University (1978).
25. D. S. Stone, et al., "Preliminary Results on the Versator Tokamak," Tech Report, RLE-117, MIT, Res. Lab. Elect., January, 1976, Cambridge, Mass.
26. G. J. Greene and R. W. Gould, Bull. Am. Phys. Soc., 26, 931 (1981).
27. S. Knox, "Phase Measurements of Fast Wave Toroidal Eigenmodes," Ph.D. Dissertation, Dept. of Elect. Engr., Texas Tech University (1979).
28. T. M. Rajkumar, "Impedance Matching for Alfvén Wave Couplers," M.S. Thesis, Dept. of Elec. Engr., Texas Tech University (1983).
29. K. L. Wong, "Fast Wave Heating of Minority Ions in the Texas Tech Tokamak," M.S. Thesis, Dept. of Elec. Engr., Texas Tech University (1984).

30. H. Akiyama, et al., Rev. Sci. Instrum. 56, 1151 (1985).
31. D. L. Book, NRL Plasma Formulary (Naval Research Laboratory, Washington, D.C., 1983).
32. K. L. Wong, et al., "Numerical Studies of Minority Heating Current Drive," Tech Report, TTUPL-86-3, TTU Plasma Lab., April 1986, Lubbock, TX.
33. H. Hammen, JET Project, Private communication.
34. P. E. Stott, Bull. Am. Phys. Soc., 30, 1361 (1985).
35. R. J. Bickerton, in the Proceeding of 1986 IEEE International Conference on Plasma Science, (Saskatoon, Canada, 1986), p. 2.
36. B. L. Wright and K. F. Schoenberg, Physics Today, 39, S-63 (1986).
37. F. F. Chen, Introduction to Plasma Physics (Plenum Press, New York, 1974).

APPENDIX A: DEFINITION OF THE SAFETY FACTOR

The safety factor, q , for tokamaks is defined by ³⁷

$$q = \frac{B_t}{B_p} \frac{a}{R}$$

where B_t is the toroidal magnetic field, B_p is the poloidal magnetic field, 'a' is the minor radius, and R is the major radius. B_p/a is proportional to current density, which varies by approximately $\pm 5\%$ in the Texas Tech Tokamak. The tokamak's toroidal magnetic field, B_t , varies from its value of .5T at the poloidal axis by +39% on the high field side of the machine to -22% on the low field side of the machine.

APPENDIX B: DEFINITION OF THE SLOWING DOWN RATE

The slowing down relaxation rate is given by ³¹

$$v_s^{\alpha/\beta} = (1 + m_\alpha/m_\beta) v_o^{\alpha/\beta} (2\pi^{-1/2}) \int_0^x dt t^{1/2} e^{-t}$$

where

$$v_o^{\alpha/\beta} = 4\pi e_\alpha^2 e_\beta^2 \lambda_{\alpha\beta} n_\beta / m_\alpha^2 V_\alpha^3 \text{ sec}^{-1}$$

and

$$x^{\alpha/\beta} = m_\beta V_\alpha^2 / 2 \kappa T_\beta .$$

where κ is the Boltzmann constant, T is temperature, V is velocity, m is mass, n is particle density, λ is the Colulomb logarithm, and e is the particle charge.

For the experiment conducted the streaming particle (labeled α) is a hydrogen ion at 4 times the ion thermal velocity. The field particles (labeled β) are also hydrogen ions, but with an effective charge of 2. The streaming particle is considered to make four toroidal transits of the Texas Tech Tokamak in moving from the high field side of the machine to the low field side, traversing approximately 12 meters. In this distance, using the slow down relaxation

rate, we can calculate that the streaming particle will have slowed significantly, so as not to participate in current drive.